Nuclear deformation across the Segre chart (nuclear landscape)

Anatoli Afanasjev
Mississippi State University (MSU), USA

Covariant density functional theory (CDFT)

The nucleons interact via the exchange of effective mesons →
→ **effective Lagrangian**

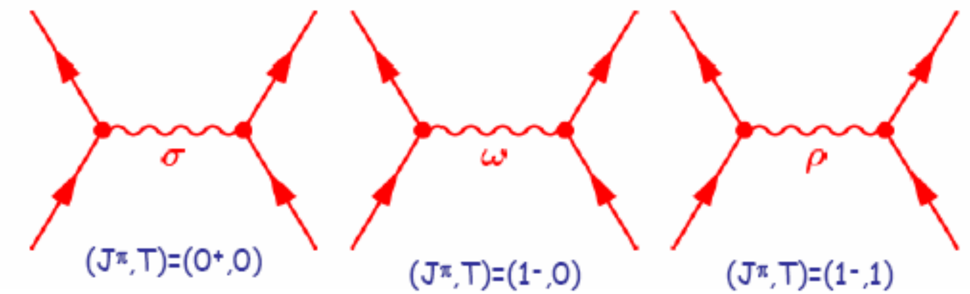

Long-range attractive scalar field

Short-range repulsive vector field

Isovector field

$$E_{\mathrm{RMF}}[\hat{\rho}, \phi_m] = \mathrm{Tr}[(\boldsymbol{\alpha p} + \beta m)\hat{\rho}] \pm \int \left[\frac{1}{2}(\nabla\phi_m)^2 + U(\phi_m)\right] \mathrm{d}^3 r + \mathrm{Tr}[(\Gamma_m \phi_m)\hat{\rho}]$$

density matrix $\hat{\rho}$ $\phi_m \equiv \{\sigma, \omega^\mu, \vec{\rho}^\mu, A^\mu\}$ - meson fields

$$\boxed{\hat{h} = \frac{\delta E}{\delta \hat{\rho}}}$$ **Mean field**

$$\boxed{\hat{h}|\varphi_i\rangle = \varepsilon_i|\varphi_i\rangle}$$ **Eigenfunctions**

Dirac equation for fermions

$$\{\vec{\alpha}\vec{p} + V + \beta(m + S)\}\,\Psi_i = \epsilon_i \Psi_i$$

$$\Psi_i = \begin{pmatrix} f_i(r) \\ i g_i(r) \end{pmatrix} = \begin{pmatrix} \text{large components} \\ \text{small components} \end{pmatrix}$$

Klein-Gordon equations for mesons

$$\{-\Delta + m_\sigma^2\}\,\sigma = -g_\sigma \rho_s - g_2\sigma^2 - g_3\sigma^3$$

$$\{-\Delta + m_\omega^2\}\,\omega_0 = g_\omega \rho_v$$

V ~ 350 MeV/nucleon
S ~ - 400 MeV/nucleon
U ~ - 50 MeV/nucleon

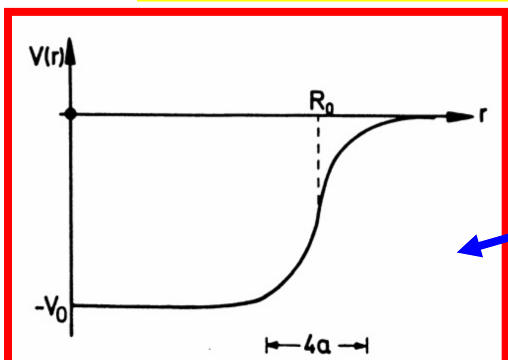

U=S+V

ω - meson

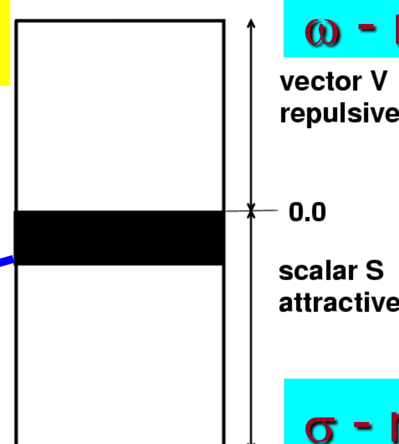

σ - meson

Densities

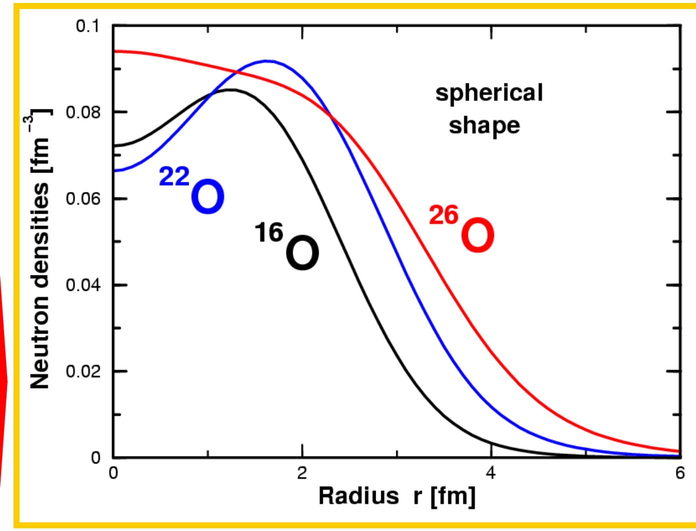

Single-particle energies

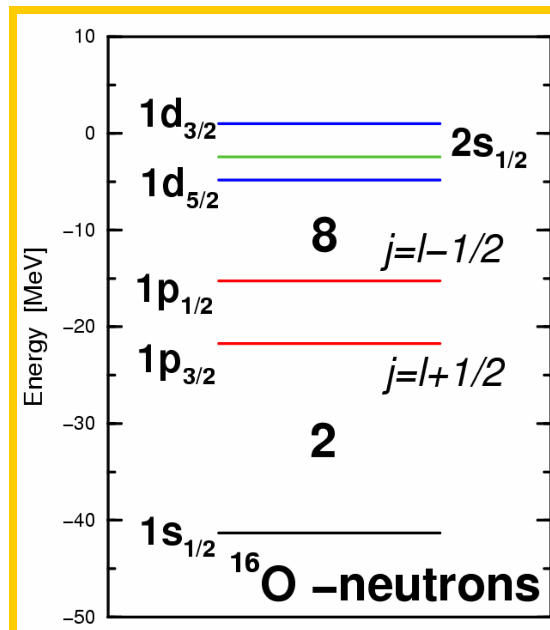

Relativistic Hartree-Bogoliubov (RHB) framework

$$\begin{pmatrix} h_D - \lambda & \Delta \\ -\Delta^* & -h_D^* + \lambda \end{pmatrix} \begin{pmatrix} U \\ V \end{pmatrix}_k = E_k \begin{pmatrix} U \\ V \end{pmatrix}_k$$

The separable version of the finite range Brink-Booker part of the Gogny D1S force is used in the particle-particle channel

$$V(\boldsymbol{r}_1, \boldsymbol{r}_2, \boldsymbol{r}_1', \boldsymbol{r}_2') =$$
$$= -f\, G\delta(\boldsymbol{R} - \boldsymbol{R}')P(r)P(r')\frac{1}{2}(1 - P^\sigma)$$

The NL3*, PC-PK1, DD-ME2, DD-PC1 and DD-MEδ covariant energy density functionals are used in order to assess the dependence of results on the functional and underlying single-particle structure and assess systematic theoretical uncertainties

The global results for even-even nuclei are available in tabulated form at:

S. Agbemava, AA, D, Ray, P.Ring, PRC **89**, 054320 (2014)
includes complete DD-PC1 mass table as supplement

Mass Explorer at FRIB (the results for DD-PC1, NL3*, DD-ME2, and DD-MEδ)
http://massexplorer.frib.msu.edu/content/DFTMassTables.html

A.V.Afanasjev, P.Ring, J. Konig, PRC 60 (1999) R051303, Nucl. Phys. A 676(2000) 196

Cranked Relativistic Hartree-Bogoliubov Theory

The CRHB equations for the fermions in the rotating frame in the one-dimensional cranking approximation

$$\begin{pmatrix} h_D - \lambda - \Omega_x \hat{J}_x & \hat{\Delta} \\ -\hat{\Delta}^* & -h_D^* + \lambda + \Omega_x \hat{J}_x \end{pmatrix} \begin{pmatrix} U_k \\ V_k \end{pmatrix} = E_k \begin{pmatrix} U_k \\ V_k \end{pmatrix}$$

Coriolis term

Klein-Gordon equations

$$\begin{aligned} \left\{-\Delta - (\Omega_x \hat{L}_x)^2 + m_\sigma^2\right\} \sigma(\boldsymbol{r}) &= -g_\sigma \rho_s(\boldsymbol{r}) - g_2 \sigma^2(\boldsymbol{r}) - g_3 \sigma^3(\boldsymbol{r}) \\ \left\{-\Delta - (\Omega_x \hat{L}_x)^2 + m_\omega^2\right\} \omega_0(\boldsymbol{r}) &= g_\omega \rho_v^{is}(\boldsymbol{r}) \\ \left\{-\Delta - (\Omega_x (\hat{L}_x + \hat{S}_x))^2 + m_\omega^2\right\} \boldsymbol{\omega}(\boldsymbol{r}) &= g_\omega \boldsymbol{j}^{is}(\boldsymbol{r}) \end{aligned}$$

Space-like components of vector mesons

currents

Important in rotating nuclei: give ~ 20-30% contr. to moments of inertia

Nuclear landscape (state-of-the-art-view)

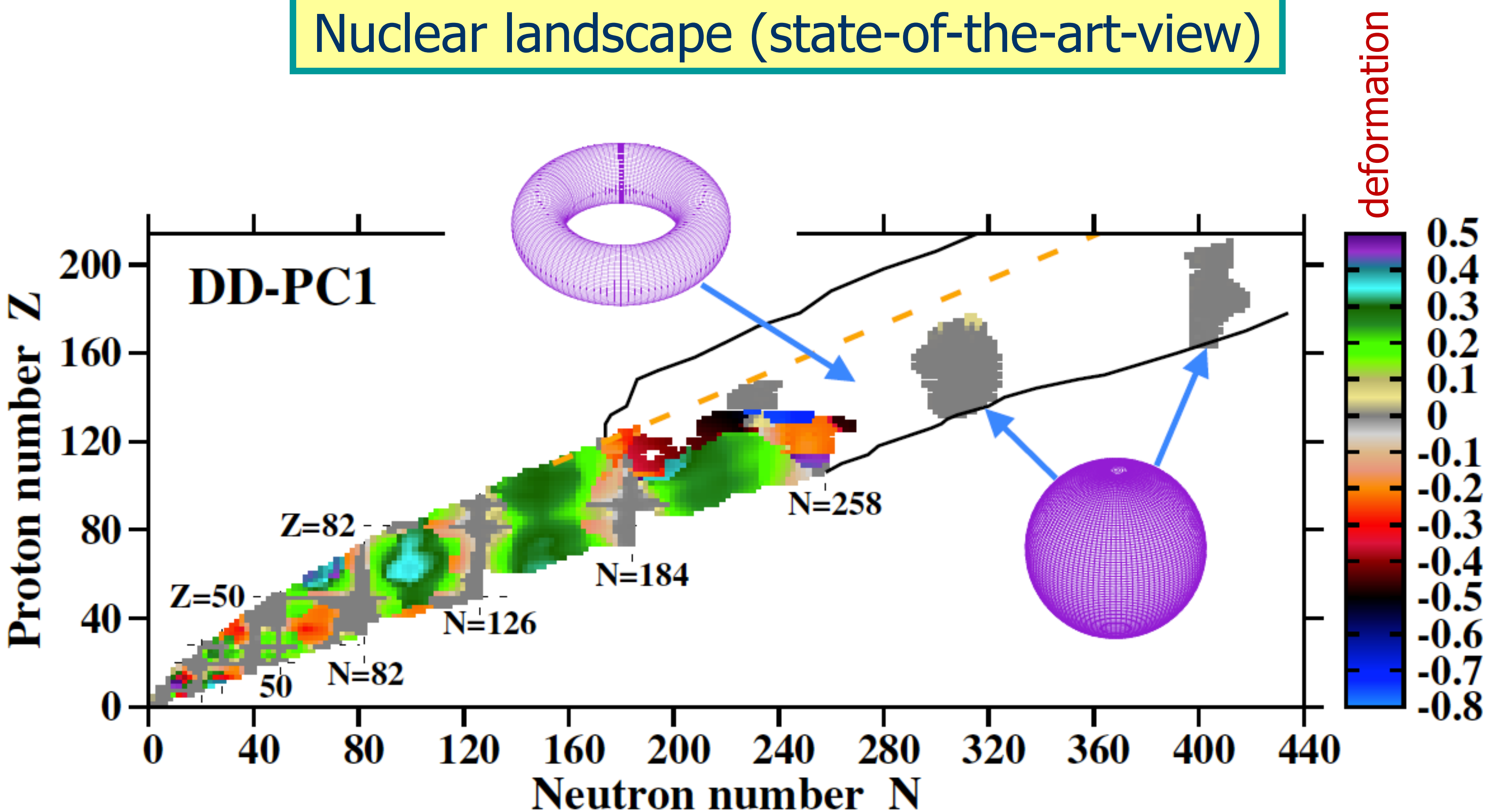

Agbemava, AA, Taninah, Gyawali,
PRC 99, 034316 (2019)
PLB 782, 533 (2018)
PRC 103, 034323 (2021)

Global description of charge radii

U.C.Perera, AA and P.Ring, PRC 104, 064313 (2021)

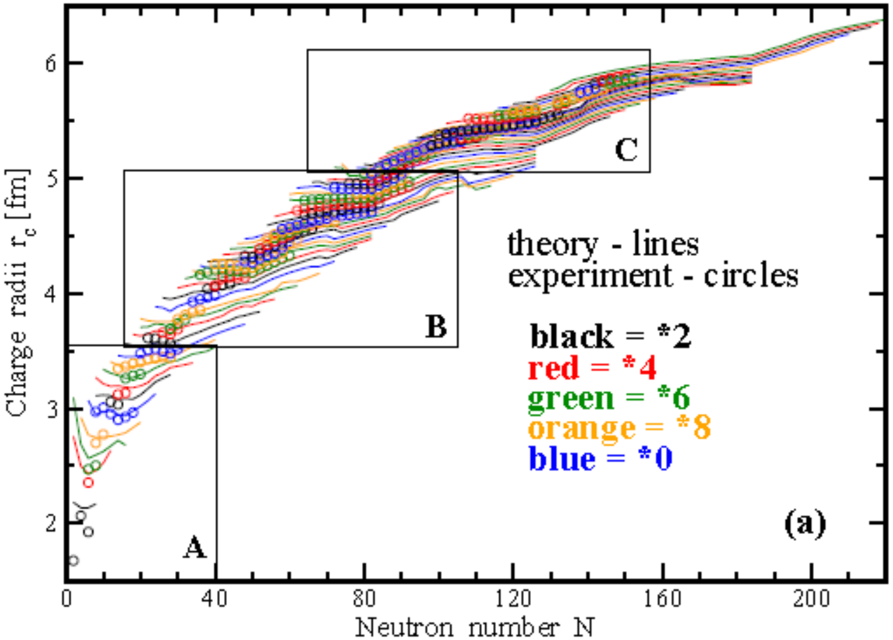

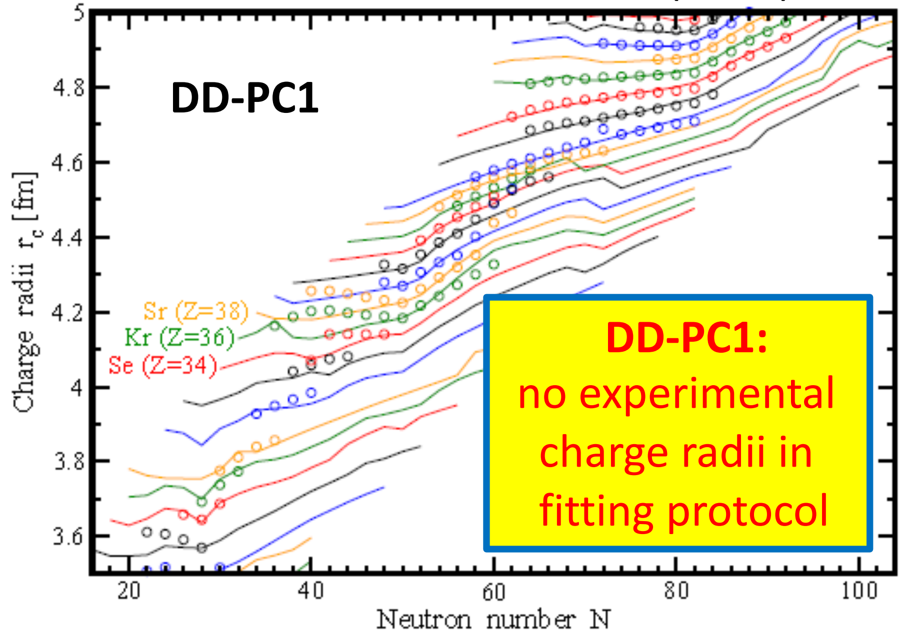

DD-PC1: no experimental charge radii in fitting protocol

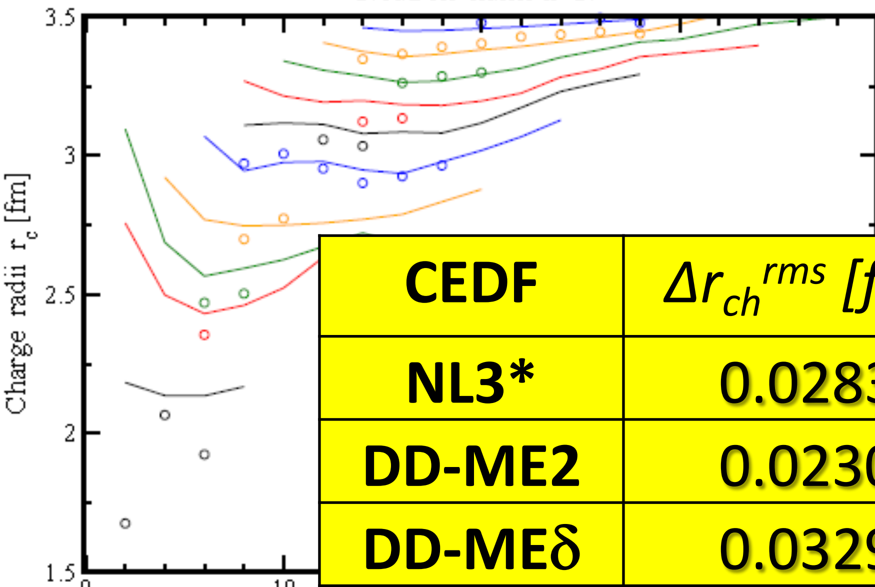

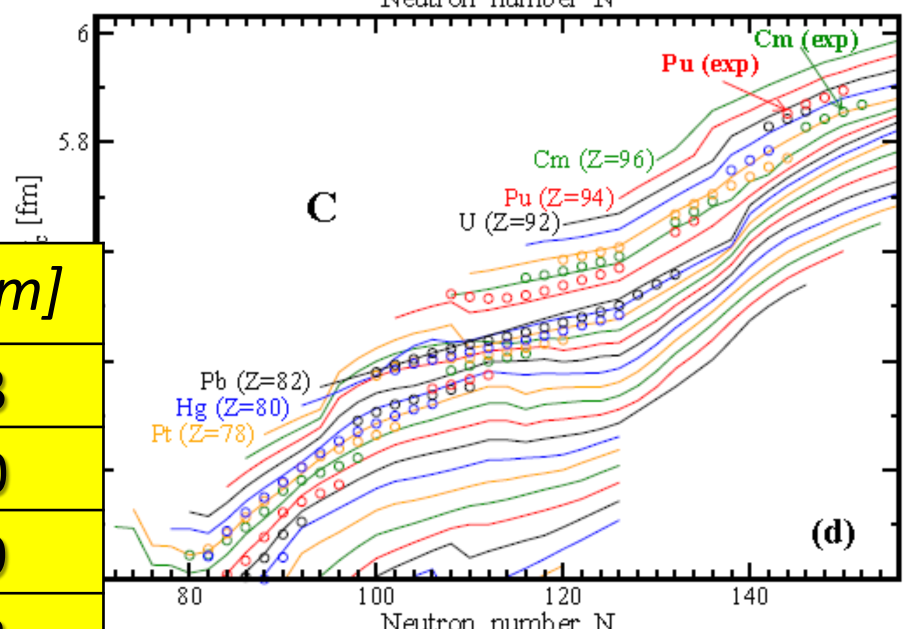

CEDF	Δr_{ch}^{rms} [fm]
NL3*	0.0283
DD-ME2	0.0230
DD-MEδ	0.0329
DD-PC1	0.0253

S. Agbemava, AA, D. Ray, P.Ring, PRC **89**, 054320 (2014) includes complete DD-PC1 mass table as supplement

Theoretical errors in the description of charge radii

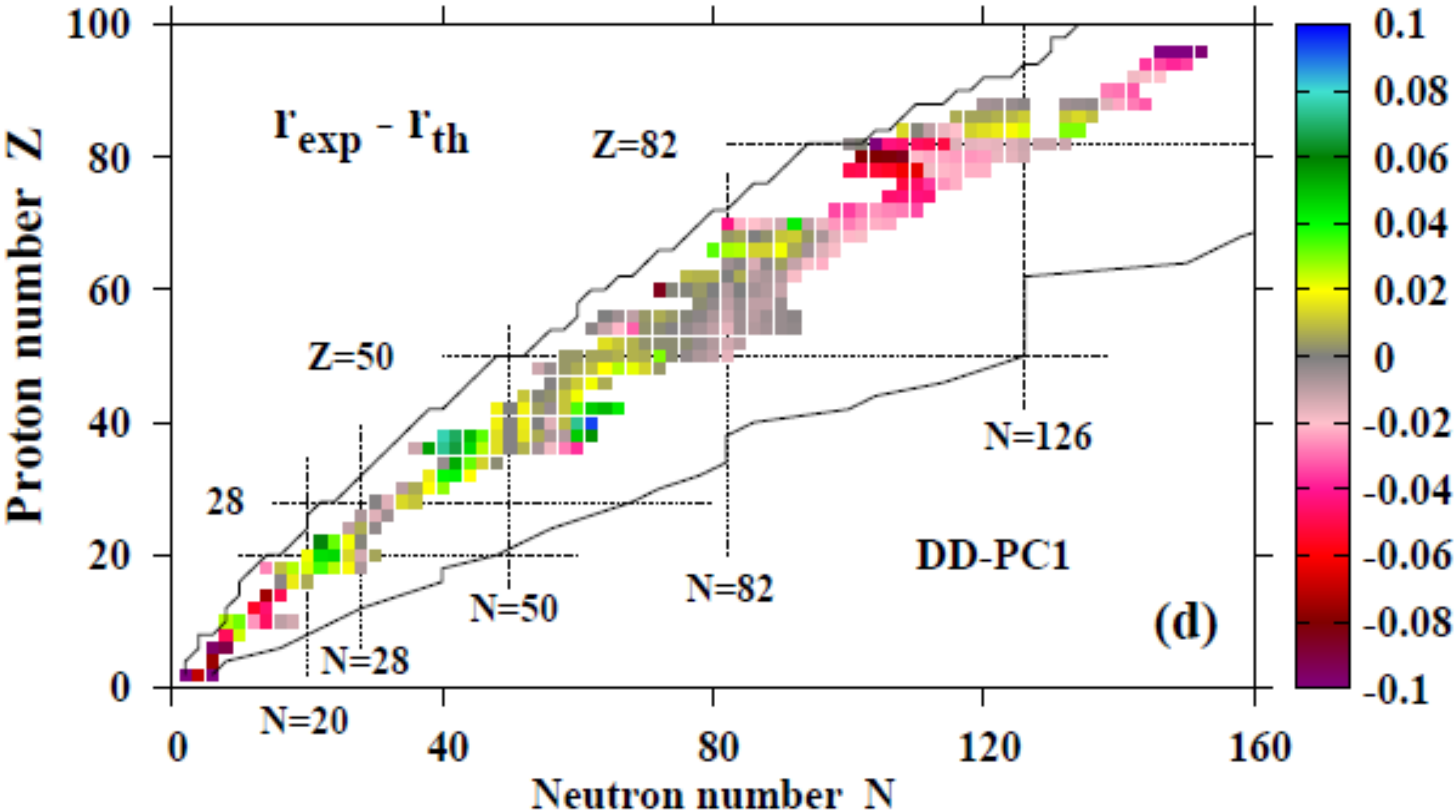

AA and S.E. Agbemava, PRC 054310 (2016)

see also U.C.Perera, AA and P.Ring, PRC 104, 064313 (2021) for more detailed investigation

Theoretical uncertainties in the description of masses

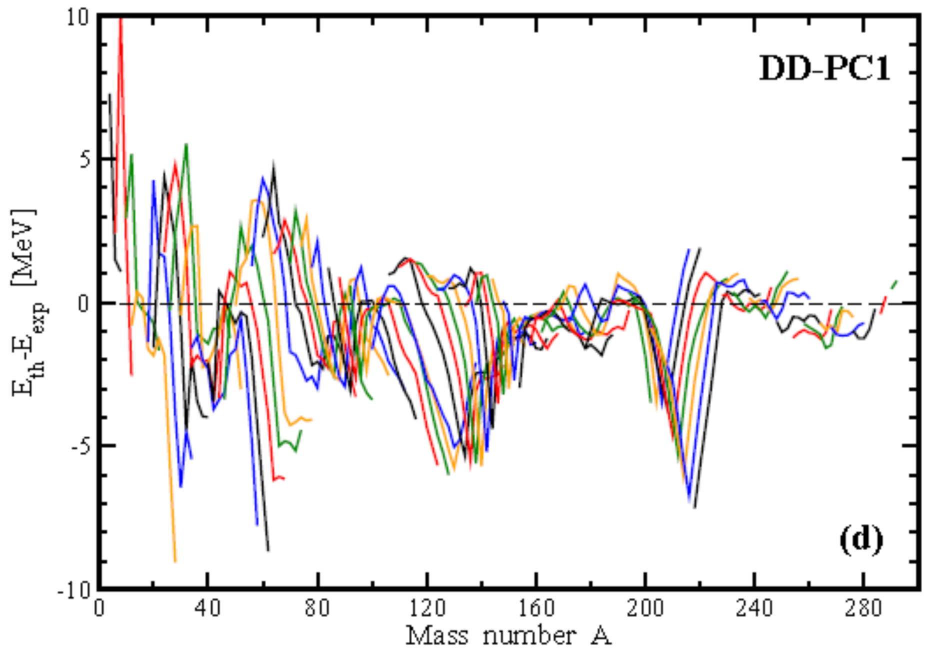

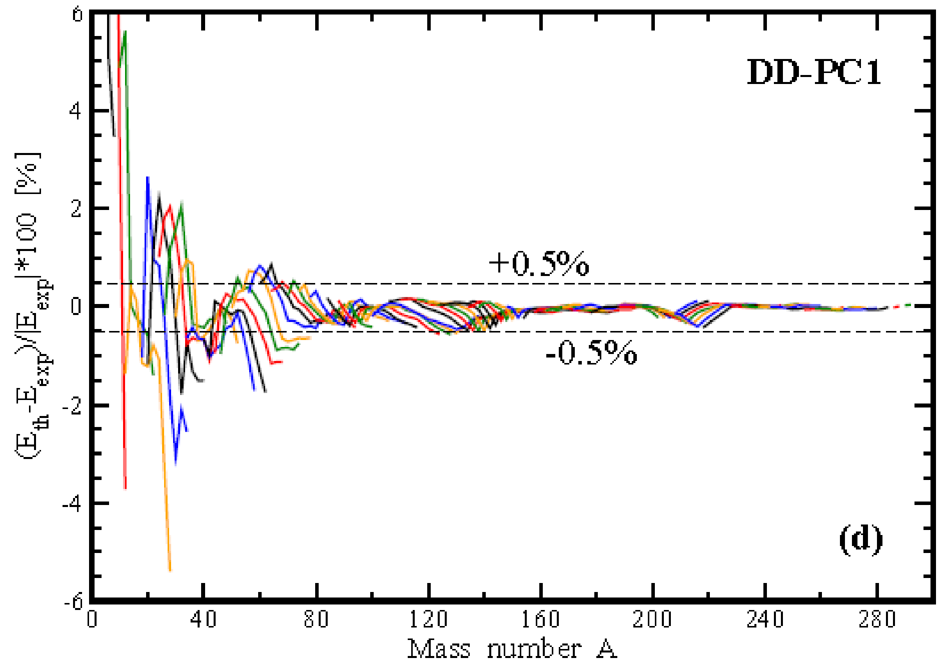

EDF	measured	measured+estimated		
	$\Delta E_{\rm rms}$	$\Delta E_{\rm rms}$	$\Delta(S_{2n})_{\rm rms}$	$\Delta(S_{2p})_{\rm rms}$
NL3*	2.96	3.00	1.23	1.29
DD-ME2	2.39	2.45	1.05	0.95
DD-MEδ	2.29	2.40	1.09	1.09
DD-PC1	2.01	2.15	1.16	1.03

Uncertainties in radii

CEDF	Δr_{ch}^{rms} [fm]
NL3*	0.0283
DD-ME2	0.0230
DD-MEd	0.0329
DD-PC1	0.0253

S. Agbemava, AA, D, Ray, P.Ring, PRC **89**, 054320 (2014)
includes complete DD-PC1 mass table as supplement

Deformation parameters and nuclear shapes

Quadrupole deformation parameter:

$$\beta_2 = Q_{20} \Big/ \left(\sqrt{\frac{16\pi}{5}} \frac{3}{4\pi} A R_0^2 \right)$$

Octupole deformation parameter:

$$\beta_3 = Q_{30} \Big/ \left(\sqrt{\frac{16\pi}{7}} \frac{3}{4\pi} A R_0^3 \right)$$

where $R_0 = 1.2 A^{1/3}$

Hexadecapole deformation parameter:

$$Q_{40} = 8\sqrt{\frac{4\pi}{9}} \frac{3}{4\pi} Z R_0^4 \beta_4$$

Multipole moments

$$Q_{20} = \langle 2z^2 - x^2 - y^2 \rangle,$$

$$Q_{30} = \langle z(2z^2 - 3x^2 - 3y^2) \rangle$$

Axial symmetric shapes: $\boldsymbol{\beta_3 = 0}$

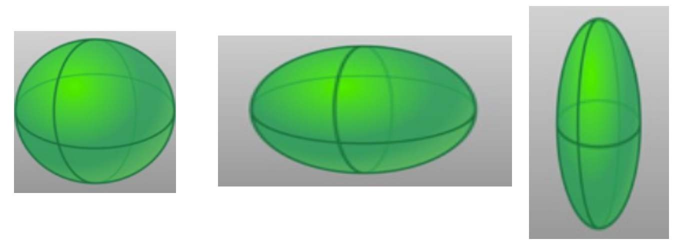

Spherical $\boldsymbol{\beta_2 = 0}$

Prolate $\boldsymbol{\beta_2 > 0}$

Oblate $\boldsymbol{\beta_2 < 0}$

Axial asymmetric (octupole) shapes: $\boldsymbol{\beta_2 \neq 0,\ \beta_3 \neq 0}$

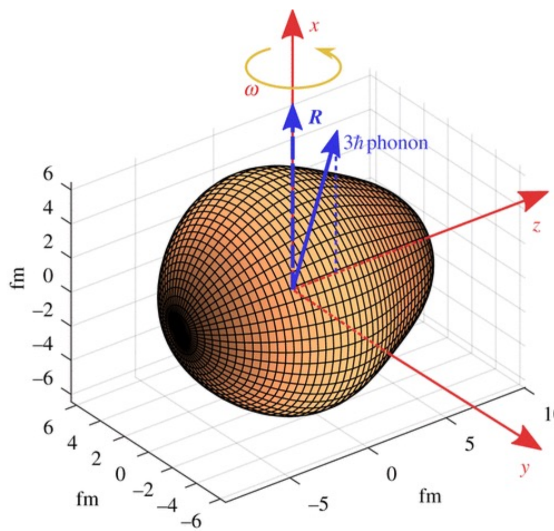

Figure from P.A.Butler, Proc.R.Soc. A476,20200202

Approximations in the modelling of nuclear many-body problem.

General approach (DFT level)

Non-relativistic Schrodinger equation:
Skyrme and Gogny DFT

Relativistic Dirac equation:
covariant DFT (CDFT)

Range of interaction

Zero range - point coupling models in CDFT (no mesons)
- Skyrme DFT

Finite range - meson exchange models in CDFT
- Gogny DFT

Effective density dependence

CDFT :
- explicit (DD-ME2, DD-PC1)
- non-linear (through the powers of mesons) (NL1, NL3*)

Skyrme and Gogny DFTs: different prescriptions for density dependence

Theoretical uncertainties:

- not well defined for the regions beyond experimentally known

A. based on the set of the models which does not form statistical ensemble

B. biases of the models are not known

→ **Systematic uncertainties**

C. biases of the fitting protocols

→ **Statistical uncertainties**

Systematic uncertainties are defined by the **spreads** (the difference between maximum and minimum values of physical observable obtained with employed set of CEDF's).

$$\Delta O(Z,N) = |O_{\max}(Z,N) - O_{\min}(Z,N)|$$

NL3*, DD-ME2, DD-MEδ, DD-PC1 and PC-PK1 functionals

How many parameters are truly independent?

NLME – class: $N_{par} = 6$

DDME – class: $N_{par} = 8$

PC – class: $N_{par} = 9$

$$\chi^2_{norm}(\mathbf{p}) = \frac{1}{s}\sum_{i=1}^{N_{type}}\sum_{j=1}^{n_i}\left(\frac{O_{i,j}(\mathbf{p}) - O^{exp}_{i,j}}{\Delta O_{i,j}}\right)^2$$

$$s = \frac{\chi^2_{norm}(\mathbf{p}_0)}{N_{data} - N_{par}}$$

Birge factor (global scale factor)

J. Dobaczewski et al, J. Phys. G,**41** (2014) 074001

$$\chi^2_{norm}(\mathbf{p}) \leq \chi^2_{norm}(\mathbf{p}_0) + \Delta\chi^2_{max}$$

	NL5(E)	DDME-X	PCPK-X
1	2	3	5
1. Masses E (MeV)			
n_1	12	12	60
ΔE [MeV]	$0.001E$	$0.001E$	1.0 MeV
2. Charge radii r_{ch} (fm)			
n_2	9	9	17
Δr_{ch} [fm]	$0.002\,r_{ch}$	$0.002\,r_{ch}$	0.02
3. Neutron skin r_{skin} (fm)			
n_3	N/A	3	N/A
Δr_{skin} [fm]	$0.05\,r_{skin}$	$0.05\,r_{skin}$	N/A
4. Nuclear matter properties			
n_4	4	4	N/A
E/A [MeV]	-16.0	-16.0	N/A
$\Delta E/A$ [MeV]	$0.05E/A$	$0.05E/A$	N/A
ρ [fm$^-3$]	0.153	0.153	N/A
$\Delta\rho$ [fm$^-3$]	0.1ρ	0.1ρ	N/A
K_0 [MeV]	250.0	250.0	N/A
ΔK_0 [MeV]	$0.025K_0$	$0.1K_0$	N/A
J [MeV]	33.0	33.0	N/A
ΔJ [MeV]	$0.1J$	$0.1J$	N/A
N_{data}	25	28	77
N_{par}	6	8	9
N_{type}	3	4	2

Parametric correlations for PC-X CEDF: Statistical analysis in full parameter hyperspace

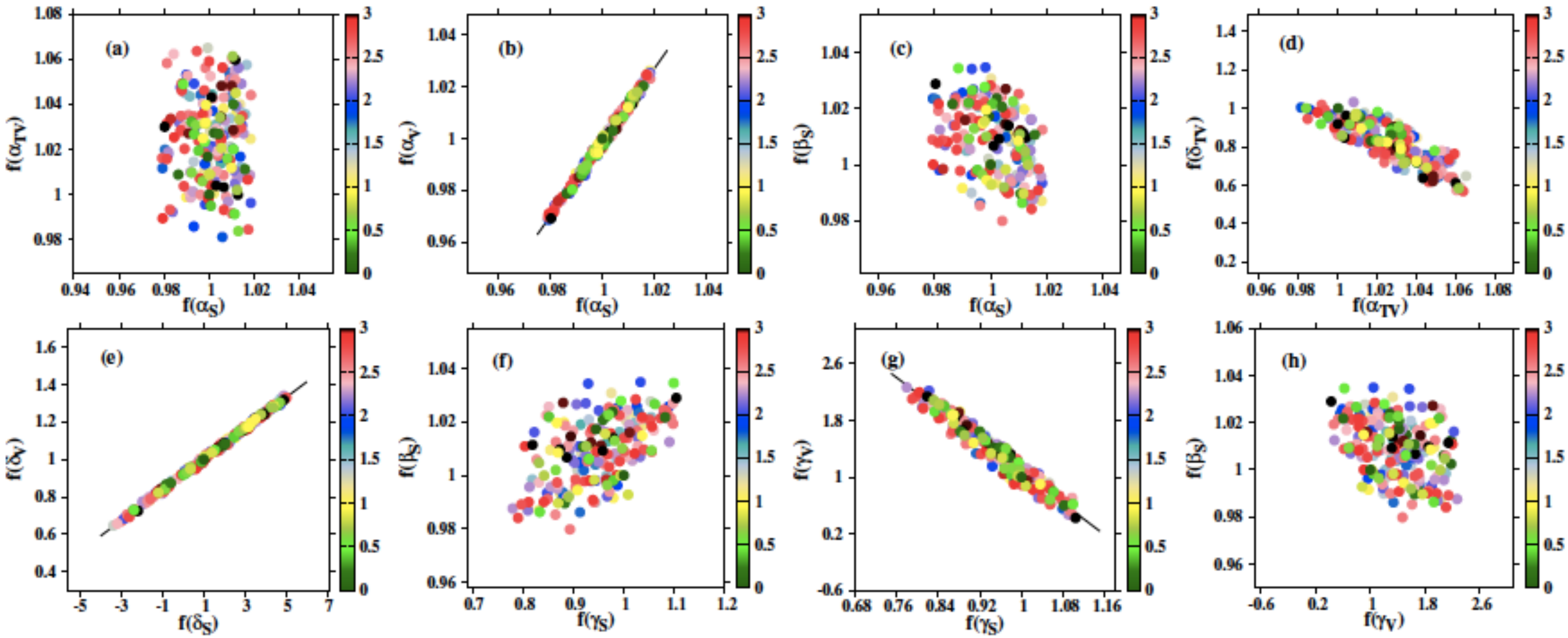

$$f(\alpha_v) = 1.4203 f(\alpha_s) - 0.42178$$

$$f(\delta_v) = 0.08221 f(\delta_s) + 0.96062$$

$$f(\gamma_v) = -5.5582 f(\gamma_s) + 6.6311$$

A.Taninah, S. Agbemava, AA, P.Ring, PLB **800**, 135065 (2020)

Proton β_2-deformation

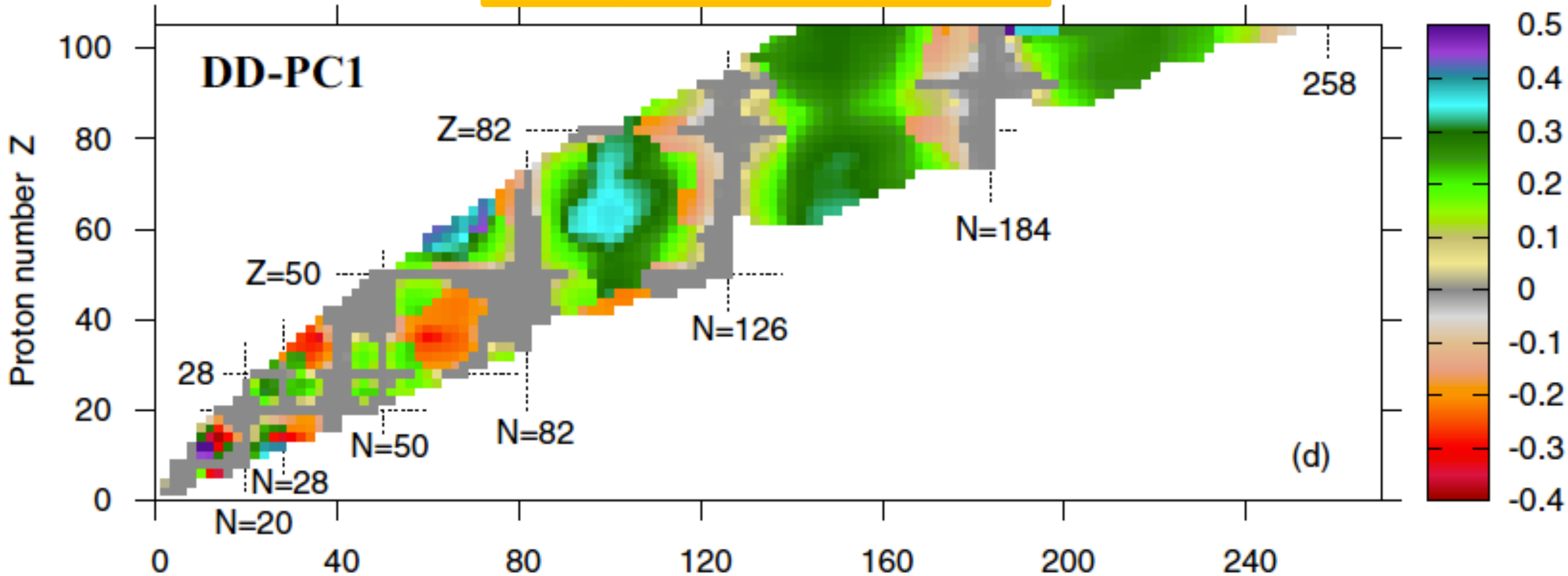

Proton hexadecapole β_4-deformation

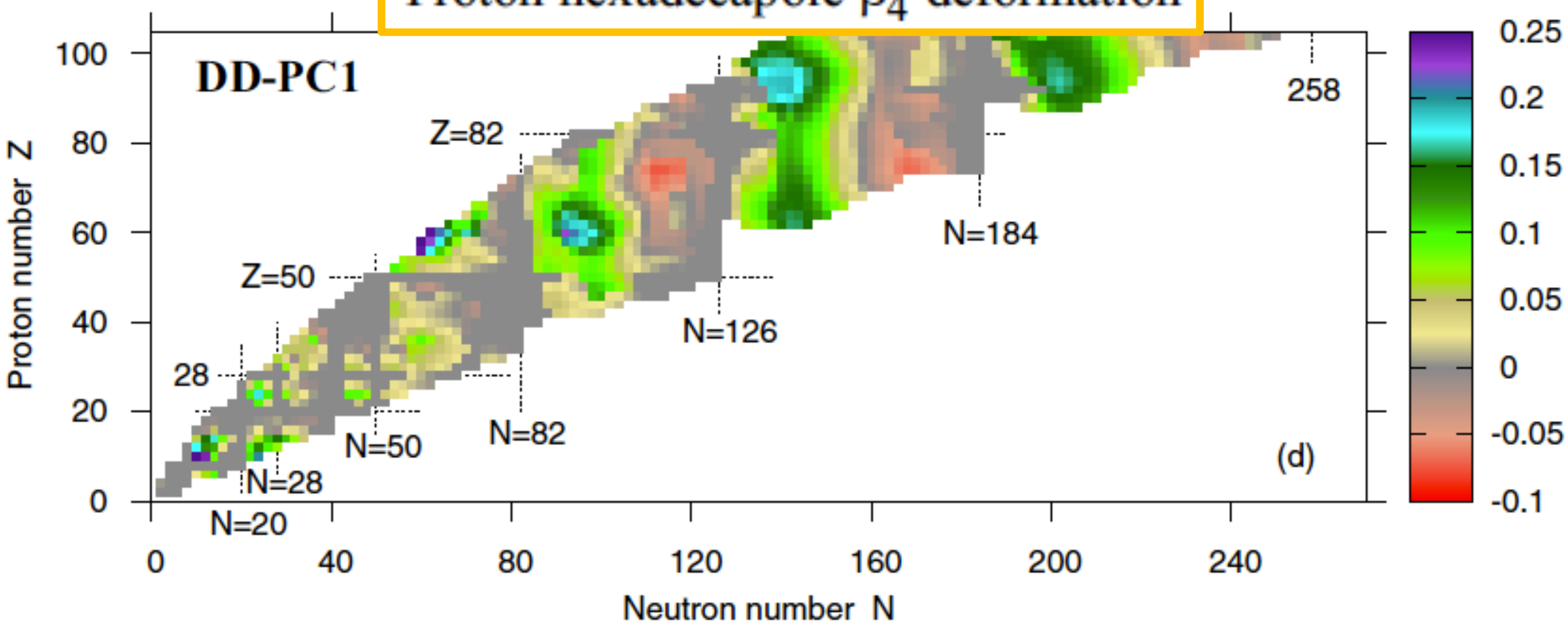

S. Agbemava, AA, D, Ray, P.Ring, PRC **89**, 054320 (2014)

Proton quadrupole deformation spread $\Delta\beta_2$

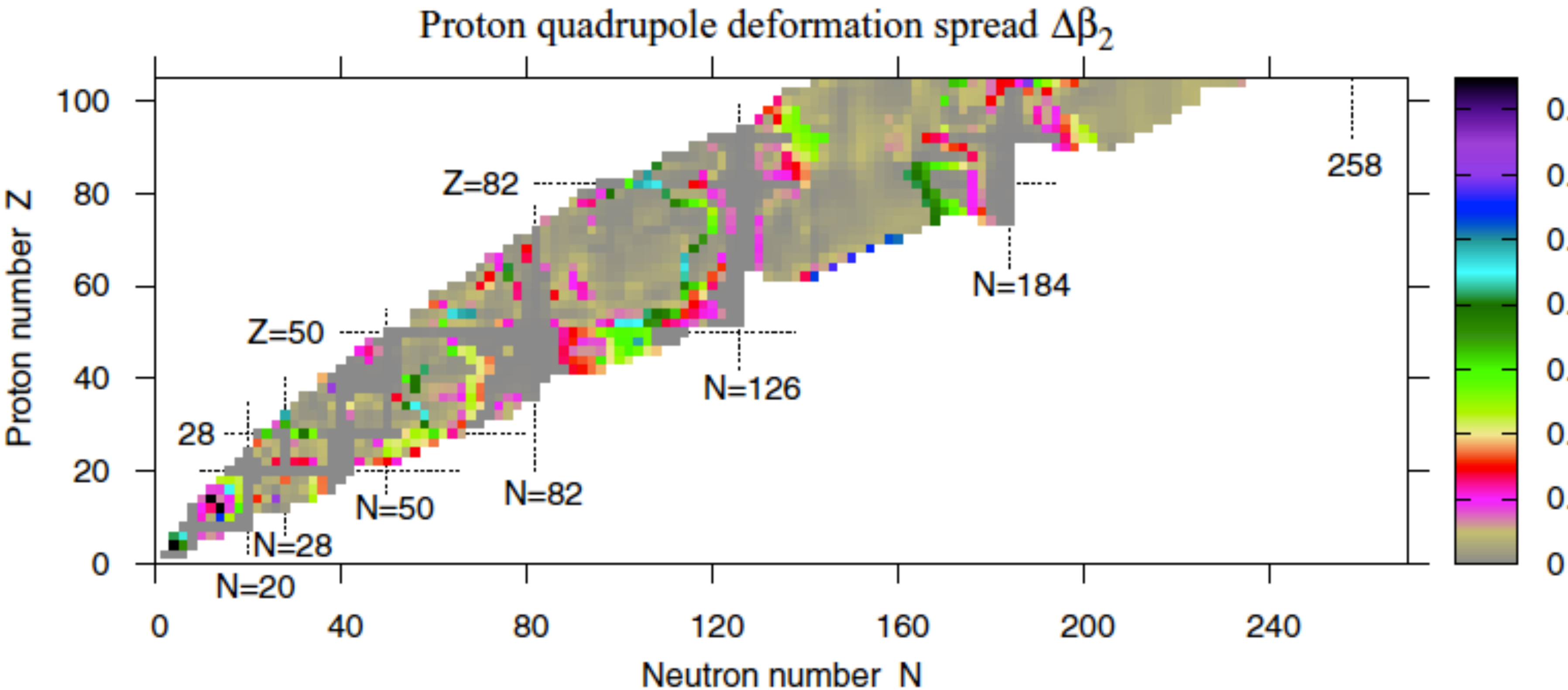

Theoretical uncertainties are most pronounced for transitional nuclei (due to soft potential energy surfaces) and in the regions of transition between prolate and oblate shapes. Details depend on the description of single-particle states

S. Agbemava, AA, D, Ray, P.Ring, PRC **89**, 054320 (2014)

Proton hexadecapole deformation spread $\Delta\beta_4$

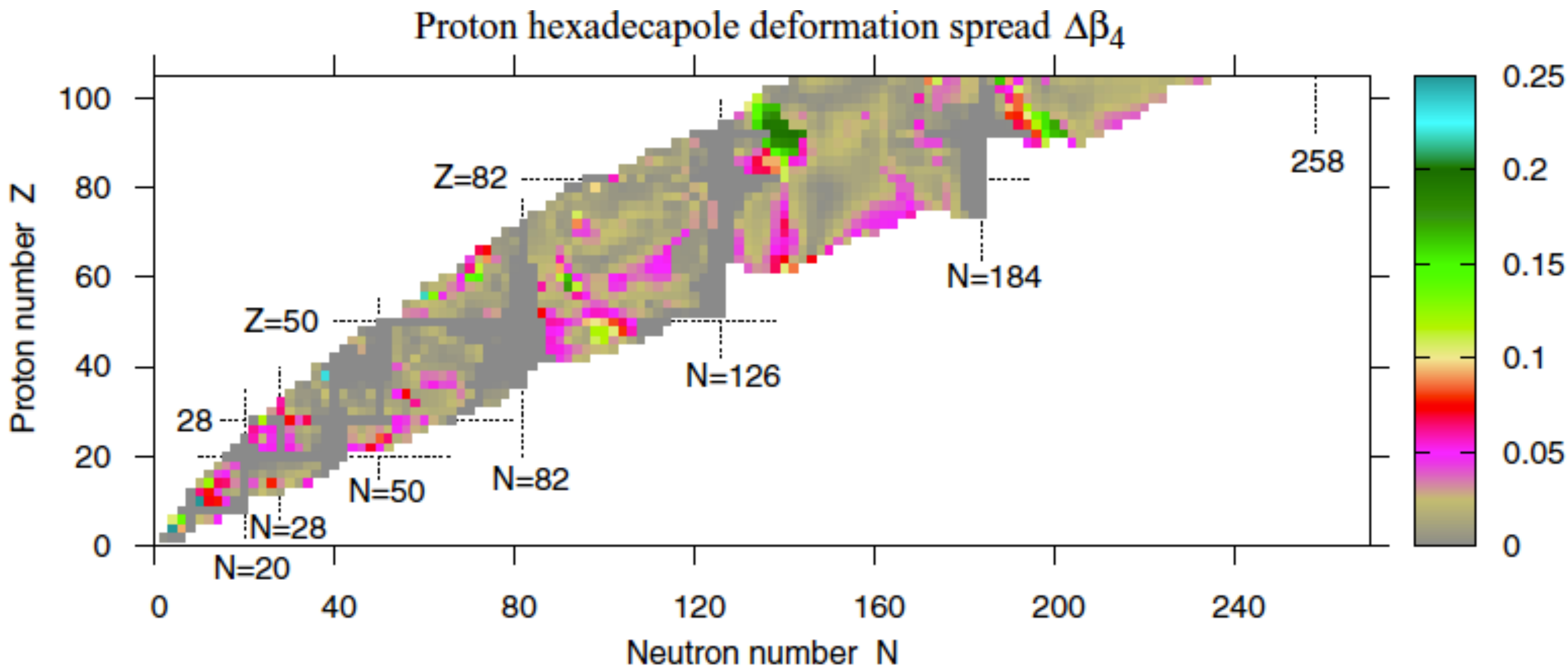

Theoretical uncertainties are most pronounced for transitional nuclei (due to soft potential energy surfaces) and in the regions of transition between prolate and oblate shapes. Details depend of the description of single-particle states

S. Agbemava, AA, D, Ray, P.Ring, PRC **89**, 054320 (2014)

$$\boxed{\text{Isovector } \beta_2^{IV} = \beta_2(\nu) - \beta_2(\pi) \text{ deformations}}$$

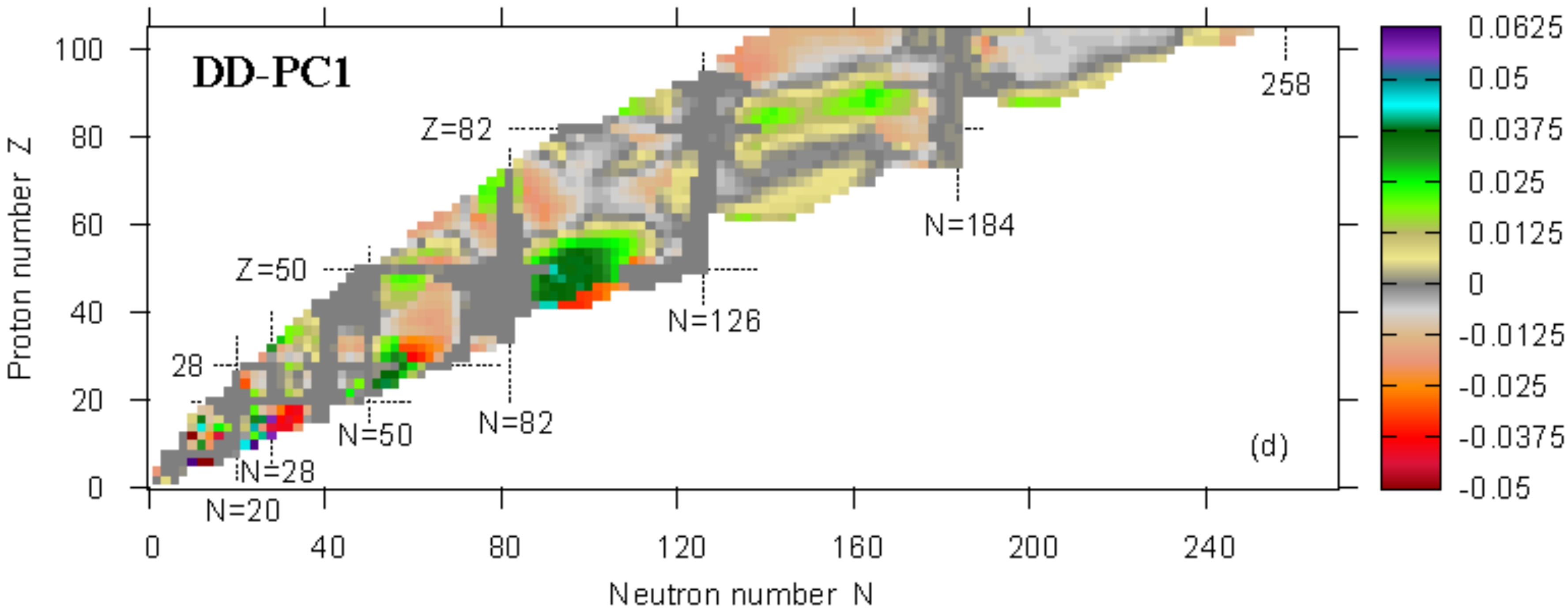

CDFT: Neutron deformation is larger than proton one in ~ 2/3 of nuclei, in the rest of deformed nuclei the situation is opposite

Skyrme DFT: Neutron deformation is smaller than proton one in majority of nuclei.

Isovector deformation is typically smaller in CDFT → **mic+mac model,** which assumes the same deformation for protons and neutrons, is **is better justified in CDFT than in Skyrme DFT.**

S. Agbemava, AA, D, Ray, P.Ring, PRC **89**, 054320 (2014)

Accuracy of the description of the single-particle states in DFTs

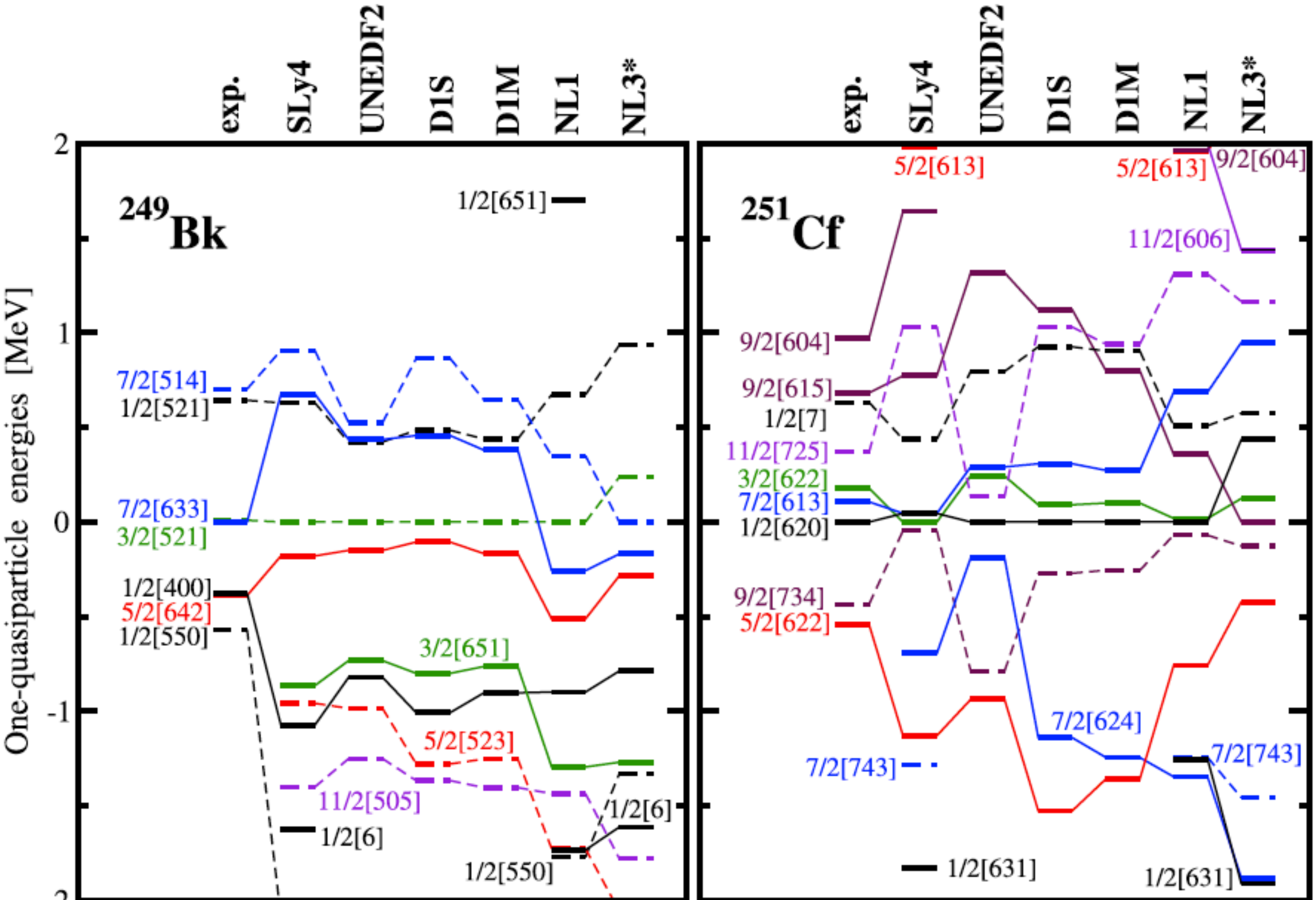

J. Dobaczewski et al, NPA 996, 388 (2015)

Systematics of one-quasiparticle states in actinides: the CRHB study

Triaxial CRHB; fully self-consistent blocking, time-odd mean fields included, Gogny D1S pairing, AA and S.Shawaqfeh, PLB 706 (2011) 177

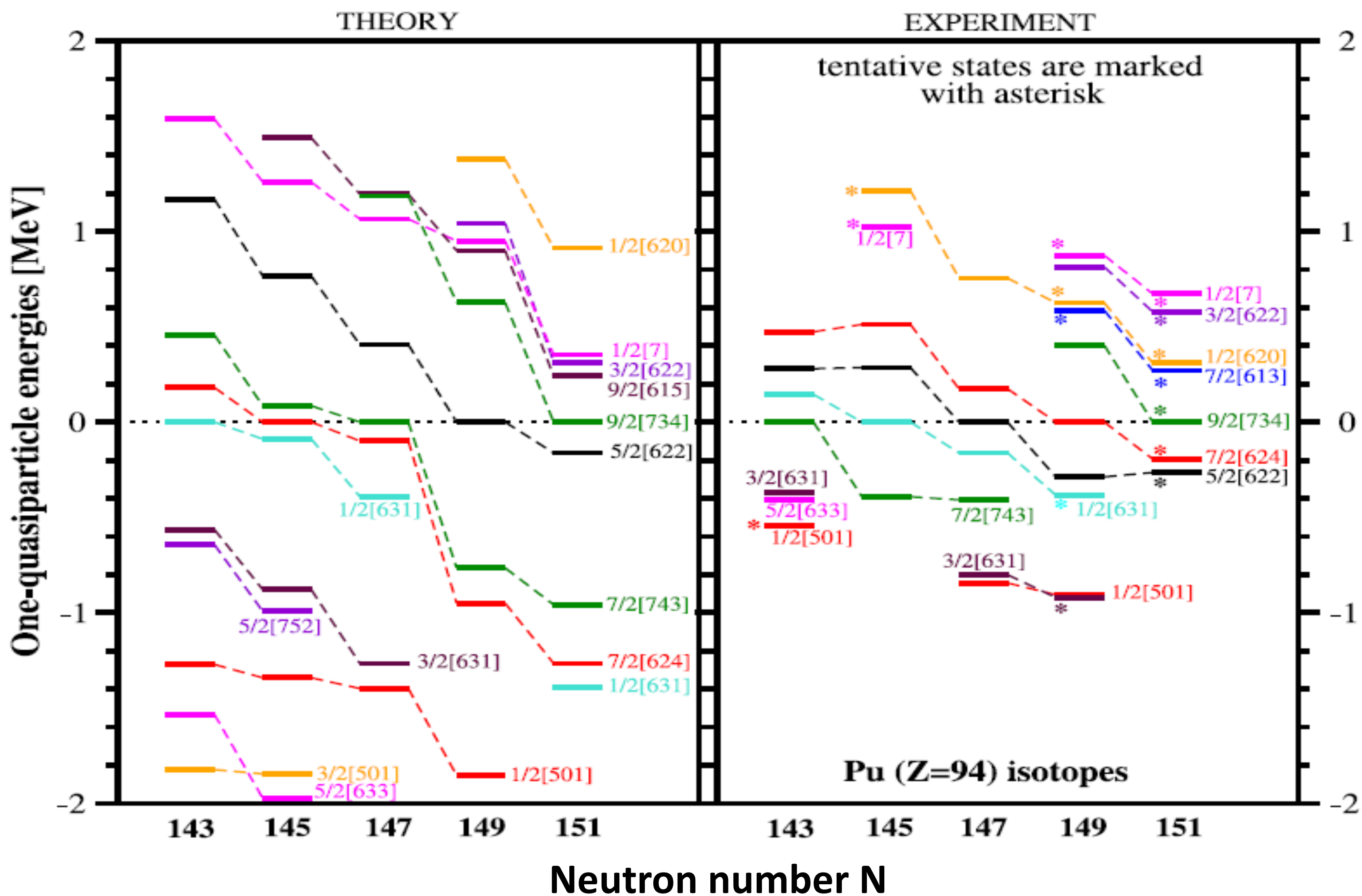

^{254}No: model dependence of the single-particle structure

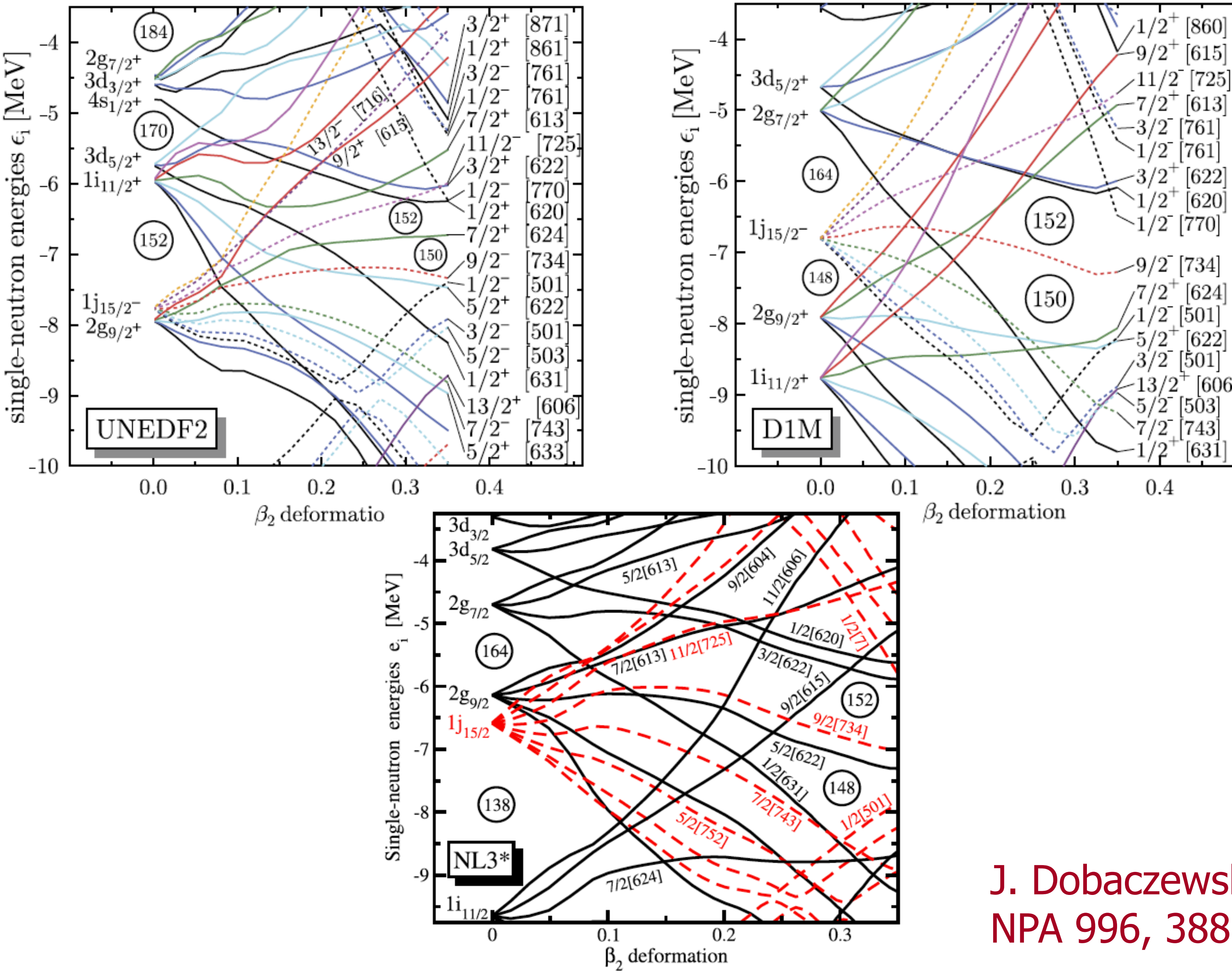

J. Dobaczewski et al, NPA 996, 388 (2015)

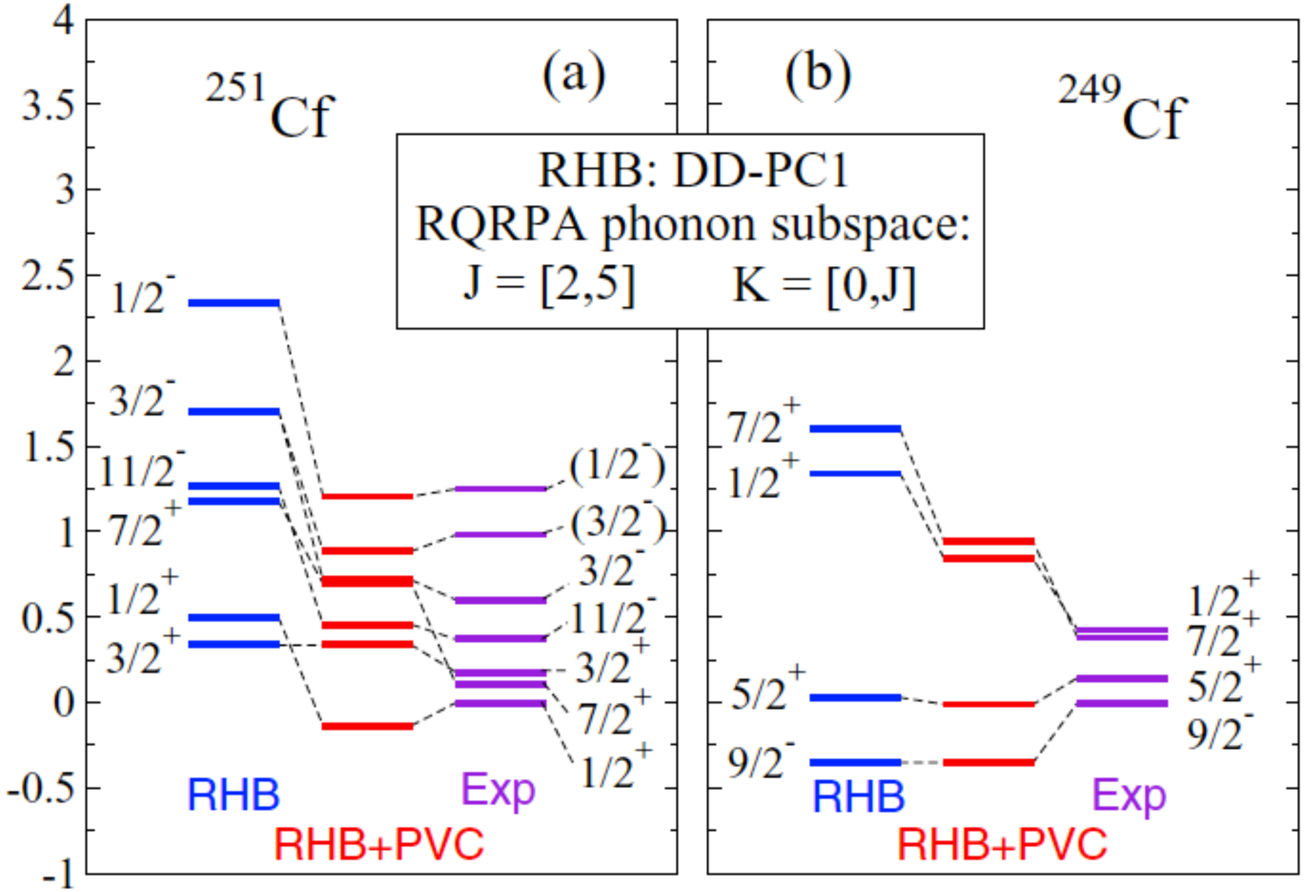

Y. Zhang et al, PRC 105, 044326 (2022)

E. Litvinova, AA, PRC 84, 014305 (2011)

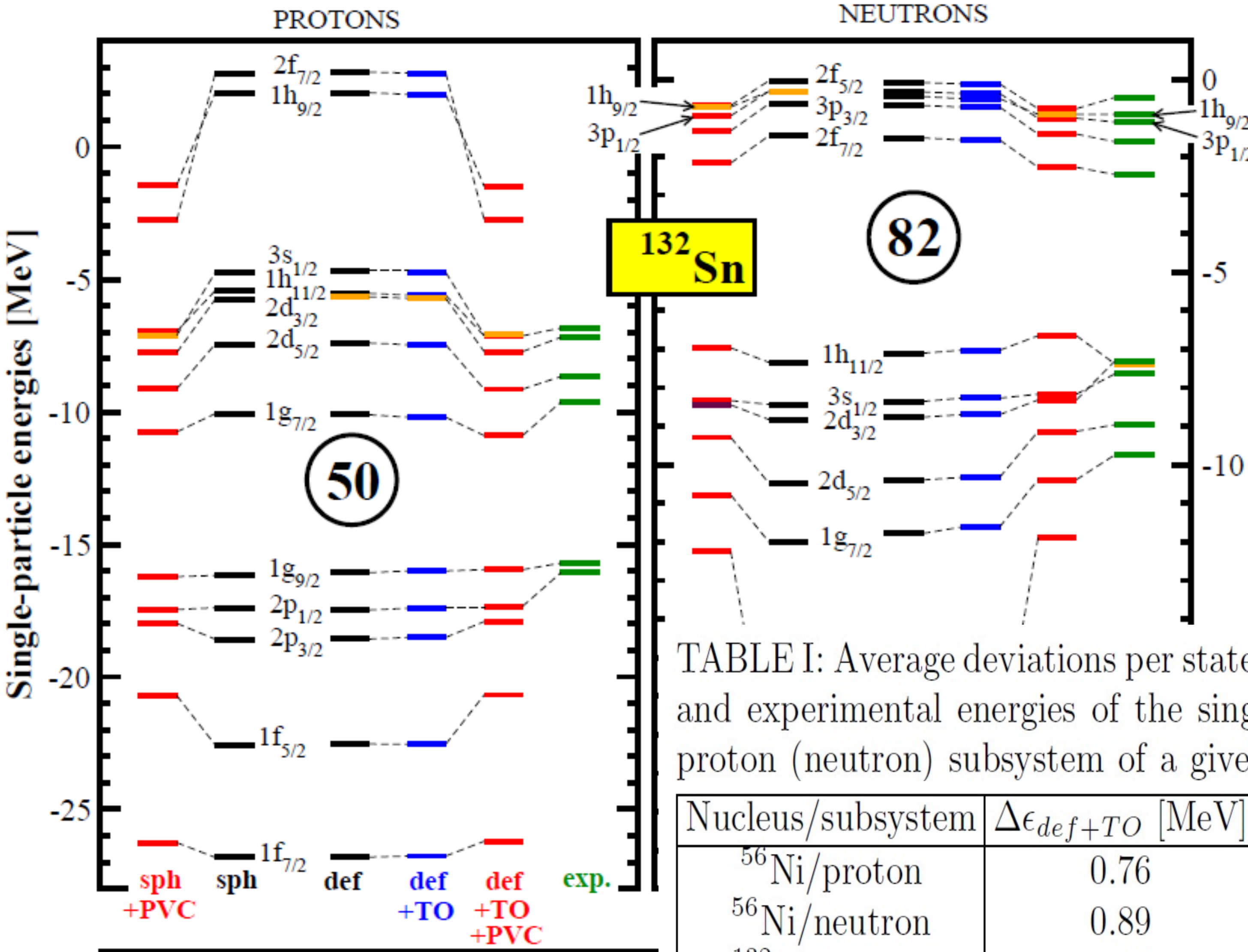

PVC – particle-vibration coupling

TABLE I: Average deviations per state $\Delta\epsilon$ between calculated and experimental energies of the single-particle states for a proton (neutron) subsystem of a given nucleus. The results

Nucleus/subsystem	$\Delta\epsilon_{def+TO}$ [MeV]	$\Delta\epsilon_{def+TO+PVC}$ [MeV]
^{56}Ni/proton	0.76	0.77
^{56}Ni/neutron	0.89	0.71
^{132}Sn/proton	1.02	0.68
^{132}Sn/neutron	0.89	0.39
^{208}Pb/proton	1.53	0.84
^{208}Pb/neutron	1.00	0.47

Deformations of the ground states in actinides states

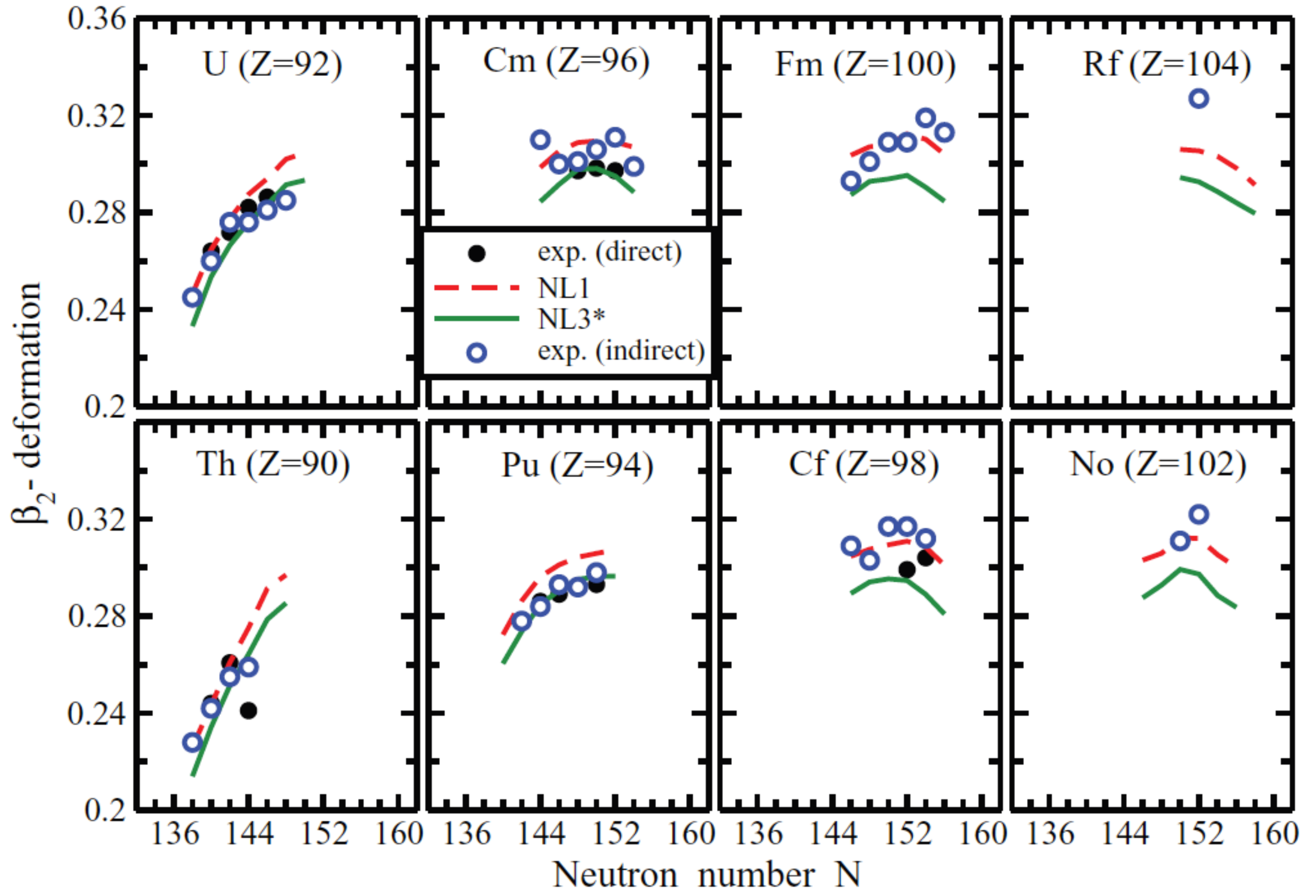

Experiment:
Direct = Coulomb excitations and lifetime measurements
Indirect = Grodzins relation

AA and O.Abdurazakov, PRC 88, 014320 (2013)

$$\beta_2 = Q_{20}/\left(\sqrt{\frac{16\pi}{5}}\frac{3}{4\pi}AR_0^2\right)$$

Note: including higher powers of β_2 yields the values of β_2 that are ~10% lower

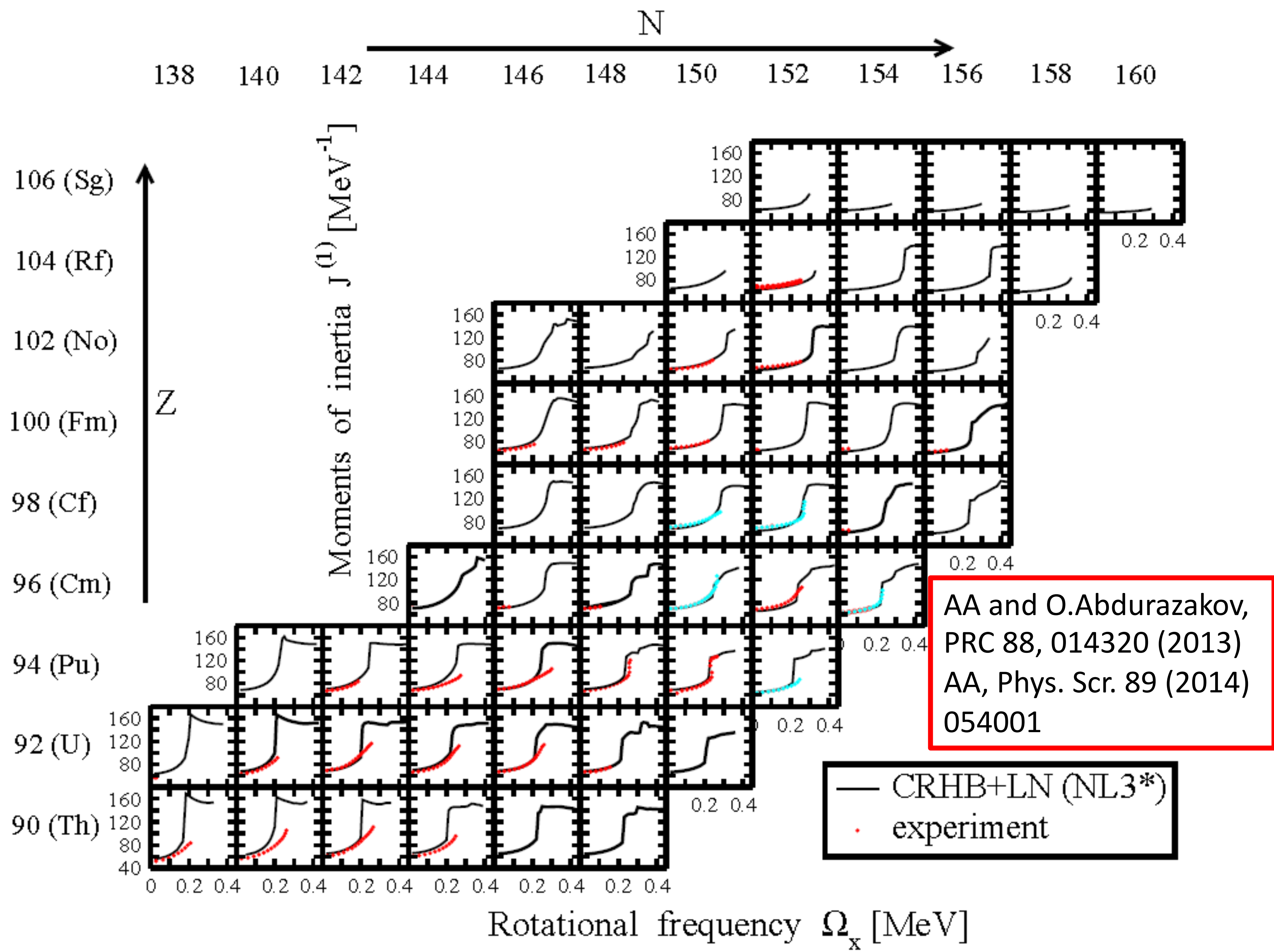
N
138
140
142
144
146
148
150
152
154
156
158
160
106 (Sg)
104 (Rf)
102 (No)
100 (Fm)
98 (Cf)
96 (Cm)
94 (Pu)
92 (U)
90 (Th)
Z
Moments of inertia J(1) [MeV-1]
Rotational frequency Ωx [MeV]
CRHB+LN (NL3*)
experiment
AA and O.Abdurazakov, PRC 88, 014320 (2013)
AA, Phys. Scr. 89 (2014) 054001

Landscape of pear-shaped even-even nuclei

Model multiplicity m(Z,N) = number of models predicting non-zero octupole deformation in the nucleus with (Z,N)

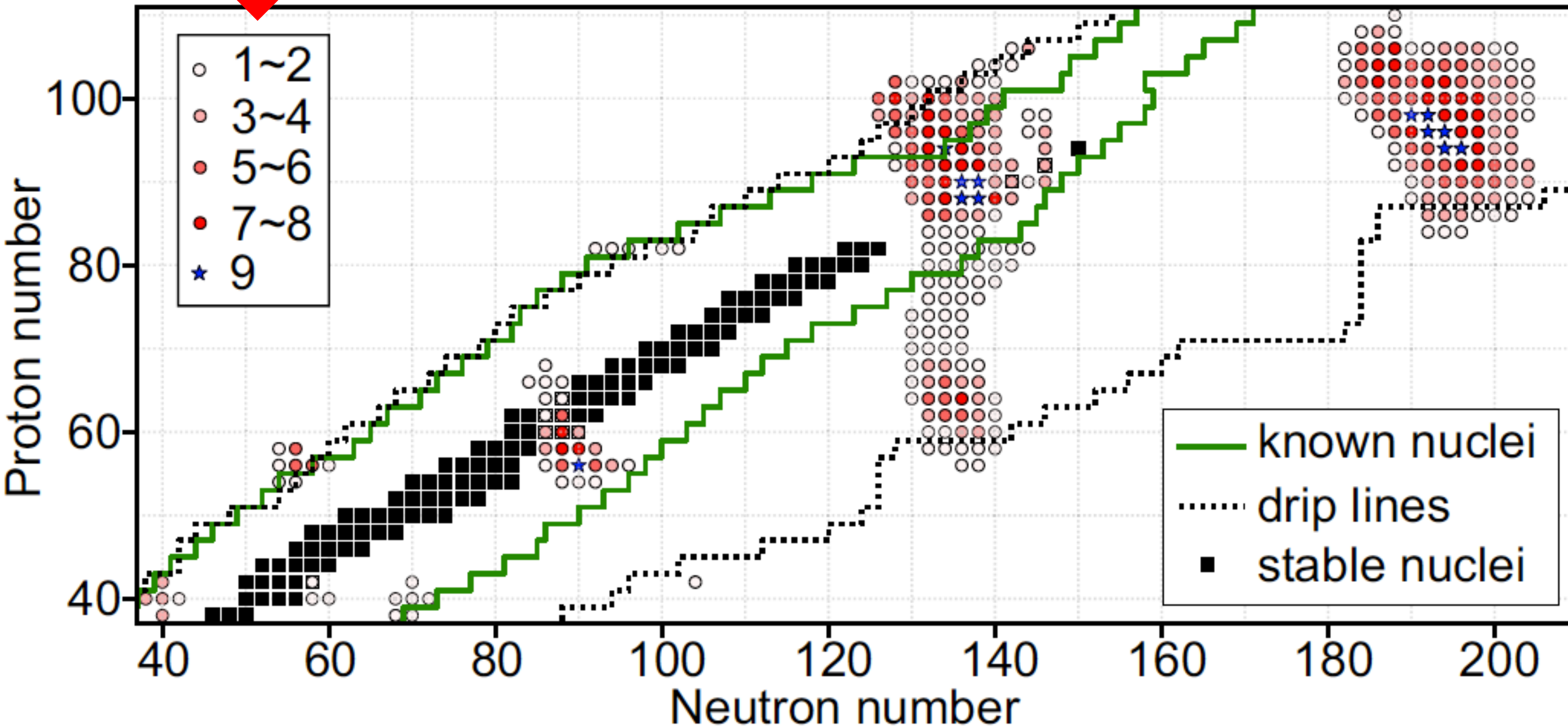

- the RHB calculations with 4 CEDFs
- Skyrme HFB calculations with 5 EDFs

Y. Cao et al, AA, PRC 102, 024311 (2020)

CDFT vs Skyrme DFT predictions for octupole deformed nuclei

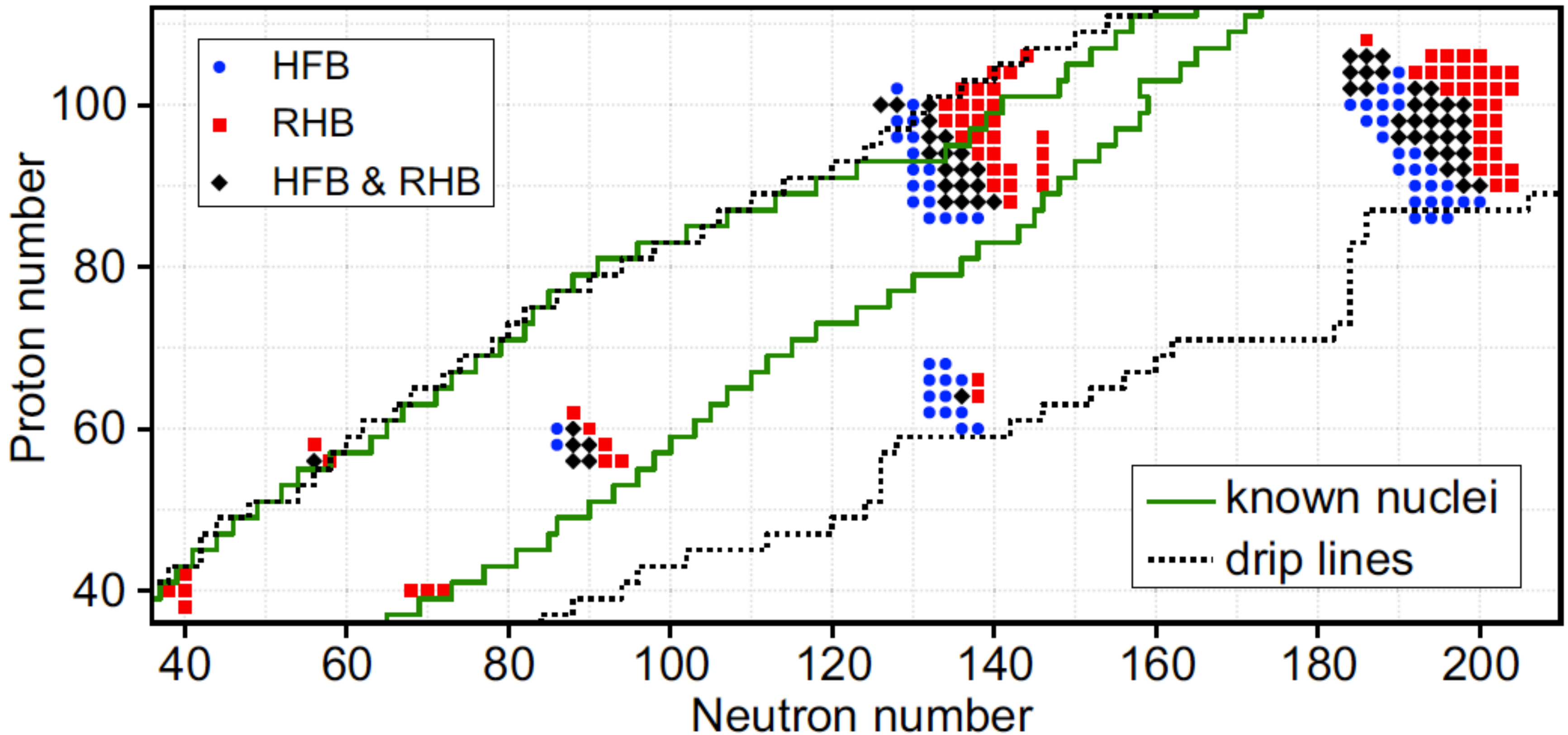

A shift in the position of octupole deformed regions (by two to four neutron numbers) is seen when comparing the results of CDFT and SDFT calculations. It comes from the differences In the underlying single-particle structure

Y. Cao et al, AA, PRC 102, 024311 (2020)

Extreme dependence of the predictions for octupole deformation on model/functional

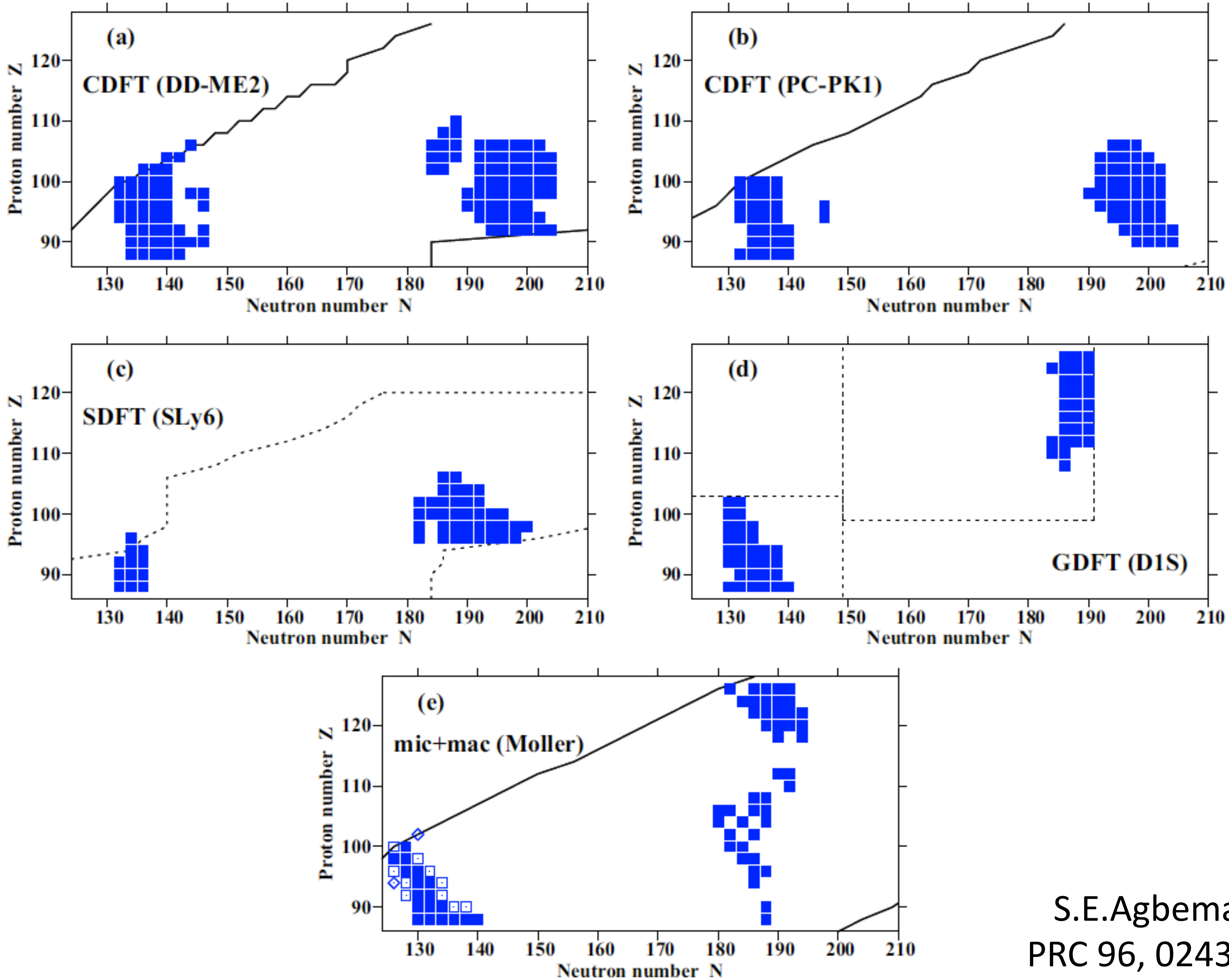

S.E.Agbemava, AA,
PRC 96, 024301 (2017)

Factors affecting the predictions of octupole deformed nuclei

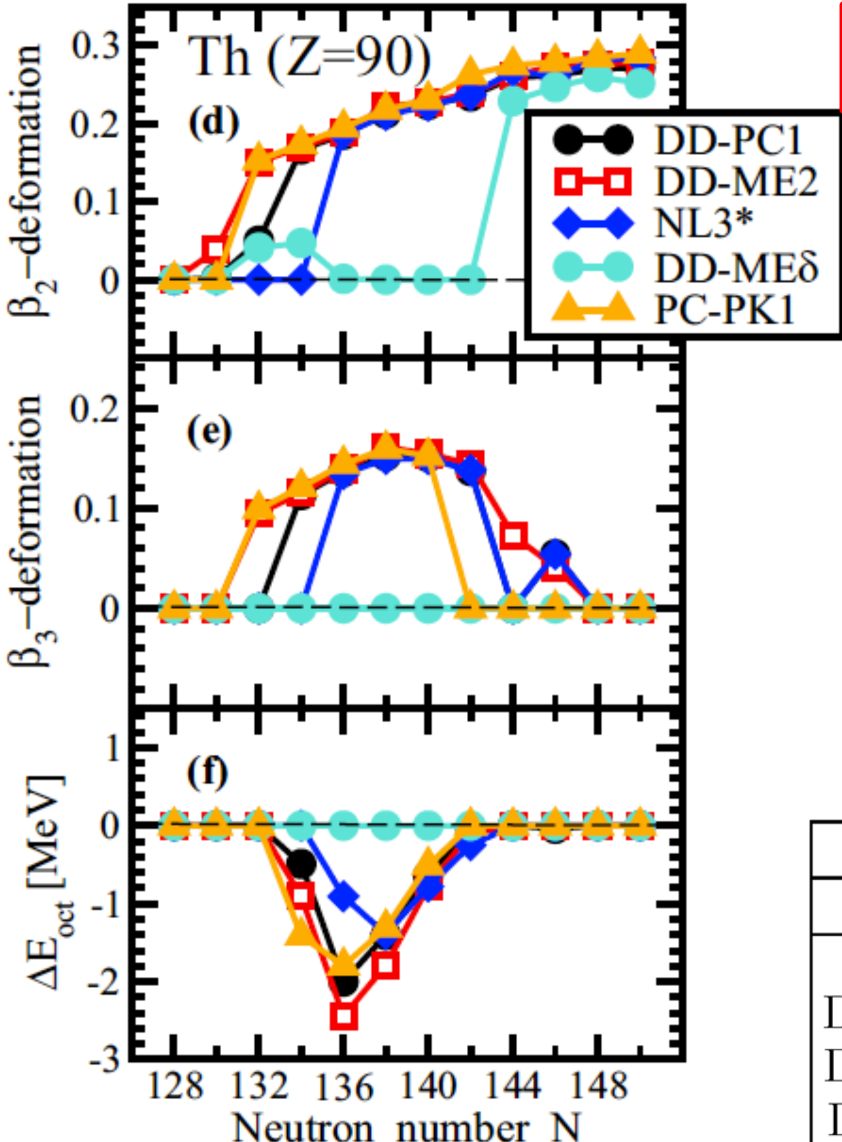

S.E.Agbemava, AA, PRC 93, 044304 (2016)

$$\Delta E_{\rm oct} = E^{\rm oct}(\beta_2,\beta_3) - E^{\rm quad}(\beta_2',\beta_3'=0)$$

The differences in the underlying single-particle structure are responsible for the differences in predictions

CEDF	Δr_{ch}^{rms} [fm]
NL3*	0.0283
DD-ME2	0.0230
DD-MEδ	0.0329
DD-PC1	0.0253

EDF	measured	measured+estimated		
	$\Delta E_{\rm rms}$	$\Delta E_{\rm rms}$	$\Delta(S_{2n})_{\rm rms}$	$\Delta(S_{2p})_{\rm rms}$
NL3*	2.96	3.00	1.23	1.29
DD-ME2	2.39	2.45	1.05	0.95
DD-MEδ	2.29	2.40	1.09	1.09
DD-PC1	2.01	2.15	1.16	1.03

S. Agbemava, AA, D, Ray, P.Ring, PRC **89**, 054320 (2014)

Factors affecting the predictions of octupole deformed nuclei: pairing

$$V(\boldsymbol{r}_1, \boldsymbol{r}_2, \boldsymbol{r}_1', \boldsymbol{r}_2') = \\ = -f\, G\delta(\boldsymbol{R}-\boldsymbol{R}')P(r)P(r')\frac{1}{2}(1-P^\sigma)$$

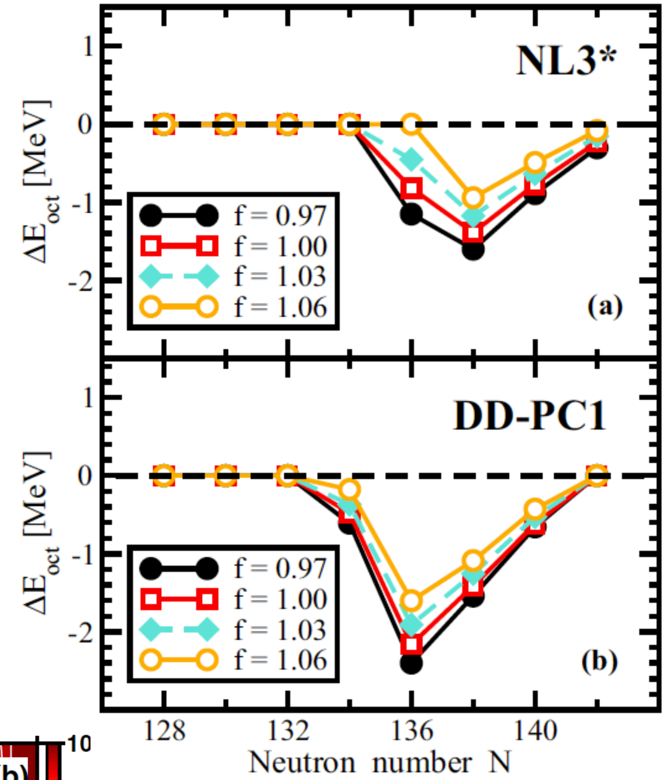

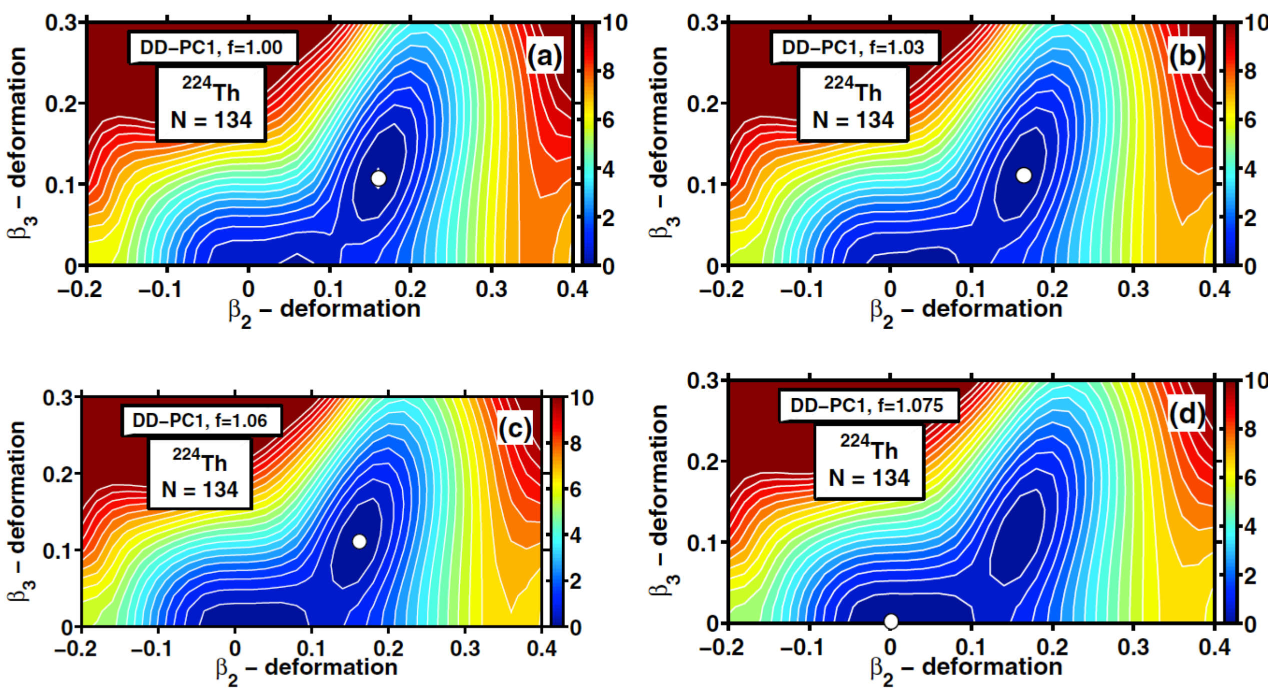

S.E.Agbemava, AA,
PRC 93, 044304 (2016)

Global study of pairing correlations indicate significant dependence of pairing strength on the way how it is extracted

$$V(\boldsymbol{r}_1, \boldsymbol{r}_2, \boldsymbol{r}'_1, \boldsymbol{r}'_2) = \\ = -f\, G\delta(\boldsymbol{R}-\boldsymbol{R'})P(r)P(r')\frac{1}{2}(1-P^\sigma)$$

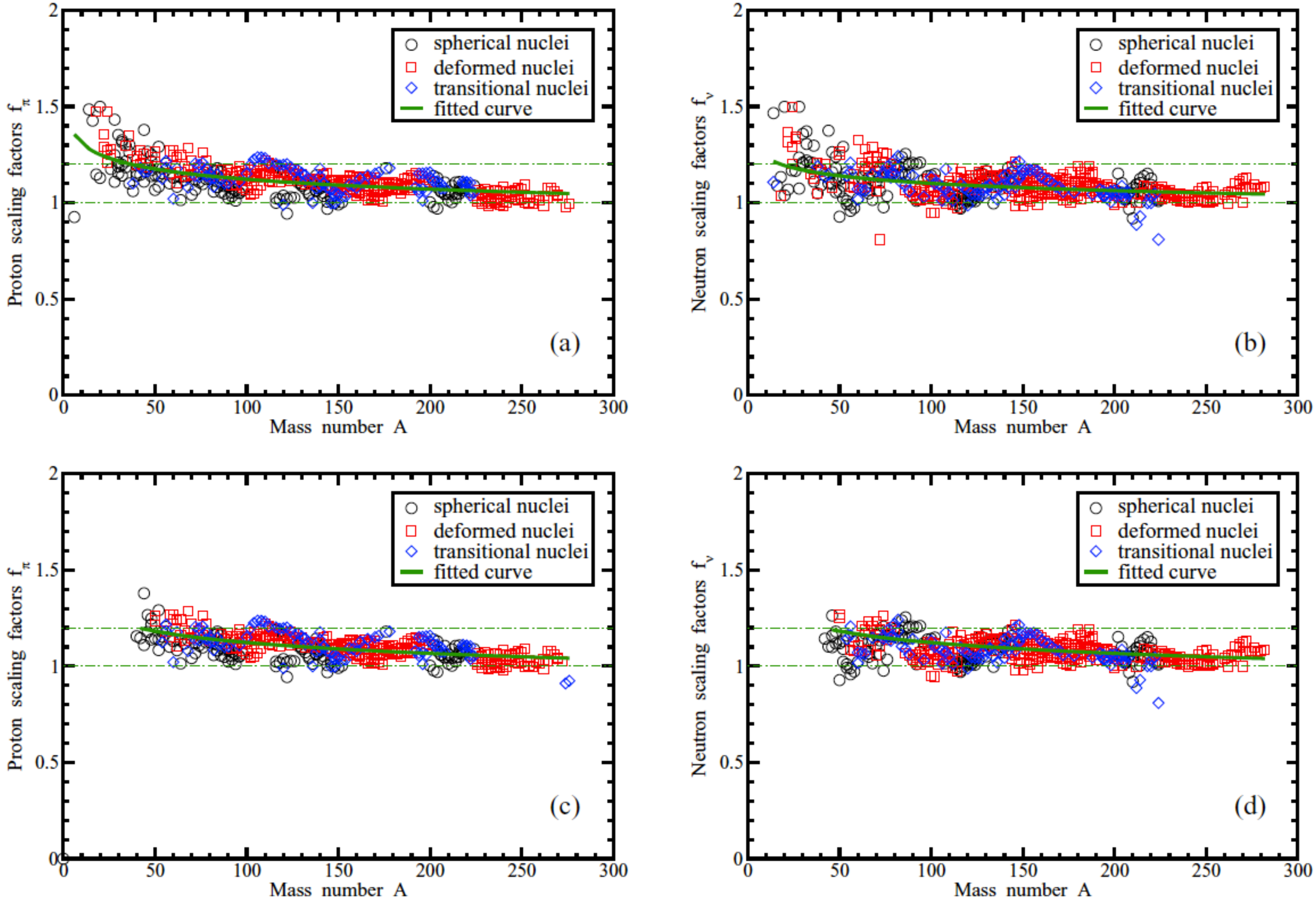

S. Teeti and AA, PRC 103, 034310 (2021)

How reliable and unique is the interpretation of ground state in ^{96}Zr

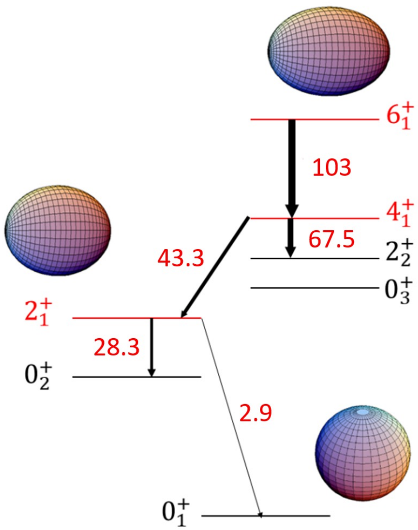

^{98}Zr: triple shape coexistence in ^{98}Zr.
ground state = spherical
PRL 121, 192501 (2018)

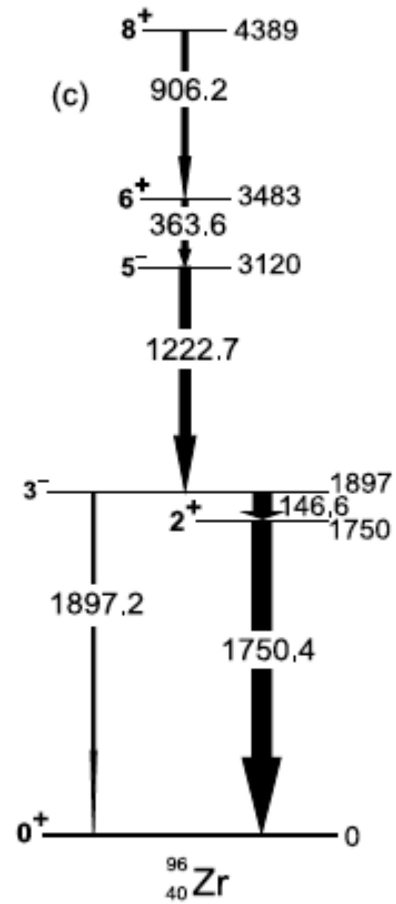

^{96}Zr: PLB 788, 396 (2019)

- reduced B(E3, $3^- \rightarrow 0^+$) strength
- Monte Carlo shell model calculations indicate that it is due to octupole vibrations

How reliable and unique is the interpretation of ground state in ^{96}Zr

Yu-Ting Rong, Bing-Nan Lu, Static octupole deformations in ^{96}Zr from angular momentum and parity projections, arXiv:2201.02114v1

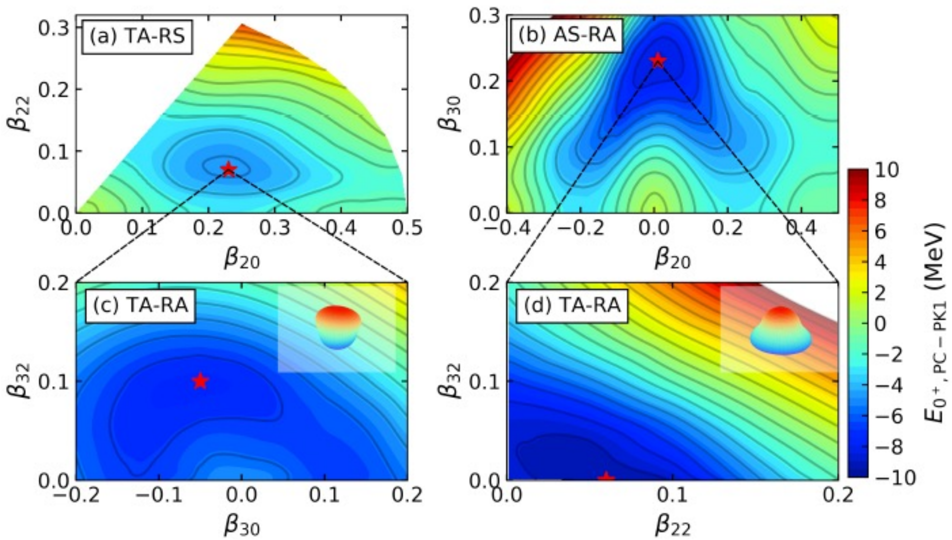

A. Petrovici and A. S. Mare, Triple shape coexistence and β decay of ^{96}Y to ^{96}Zr, PRC 101, 024307 (2020)

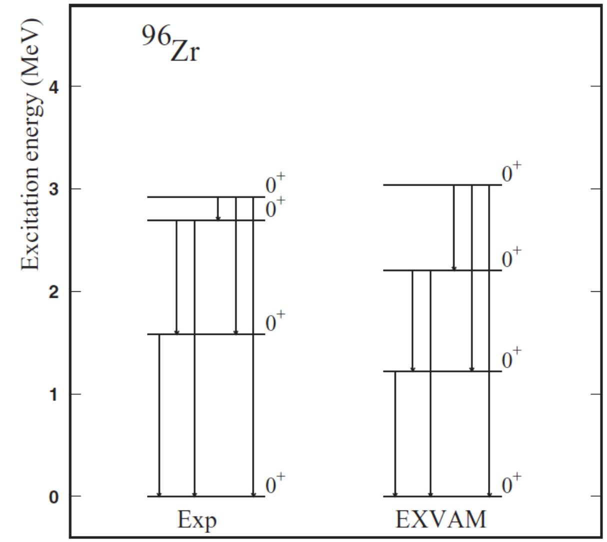

TABLE I. The structure of the wave functions for the lowest four 0^+ states of ^{96}Zr.

$I[\hbar]$	Spherical	Prolate	Oblate
0_1^+	94%	1%	4%
0_2^+	19%	45%	35%
0_3^+	30%	54%	15%
0_4^+	36%	16%	47%

Are the density distributions flat in the central region of the nuclei of interest

$$\rho(r) = \frac{\rho_0}{1 + \exp\left(\frac{r-R}{a}\right)}$$

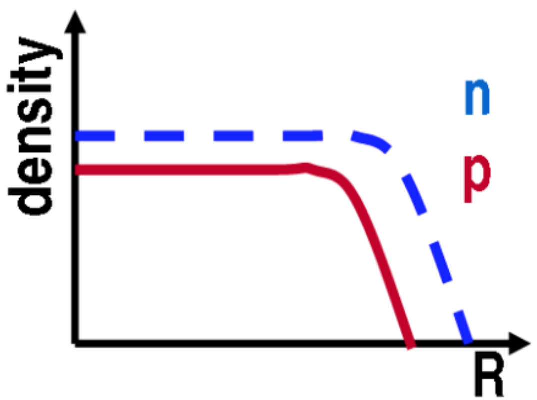

arXiv:2102.08158

A	isobars	A	isobars	A	isobars
36	Ar, S	106	Pd, Cd	148	Nd, Sm
40	Ca, Ar	108	Pd, Cd	150	Nd, Sm
46	Ca, Ti	110	Pd, Cd	152	Sm, Gd
48	Ca, Ti	112	Cd, Sn	154	Sm, Gd
50	Ti, V, Cr	113	Cd, In	156	Gd, Dy
54	Cr, Fe	114	Cd, Sn	158	Gd, Dy
64	Ni, Zn	115	In, Sn	160	Gd, Dy
70	Zn, Ge	116	Cd, Sn	162	Dy, Er
74	Ge, Se	120	Sn, Te	164	Dy, Er
76	Ge, Se	122	Sn, Te	168	Er, Yb
78	Se, Kr	123	Sb, Te	170	Er, Yb
80	Se, Kr	124	Sn, Te, Xe	174	Yb, Hf
84	Kr, Sr, Mo	126	Te, Xe	176	Yb, Lu, Hf
86	Kr, Sr	128	Te, Xe	180	Hf, W
87	Rb, Sr	130	Te, Xe, Ba	184	W, Os
92	Zr, Nb, Mo	132	Xe, Ba	186	W, Os
94	Zr, Mo	134	Xe, Ba	187	Re, Os
96	Zr, Mo, Ru	136	Xe, Ba, Ce	190	Os, Pt
98	Mo, Ru	138	Ba, La, Ce	192	Os, Pt
100	Mo, Ru	142	Ce, Nd	198	Pt, Hg
102	Ru, Pd	144	Nd, Sm	204	Hg, Pb
104	Ru, Pd	146	Nd, Sm		

Are the densities flat in the central part of the nucleus?

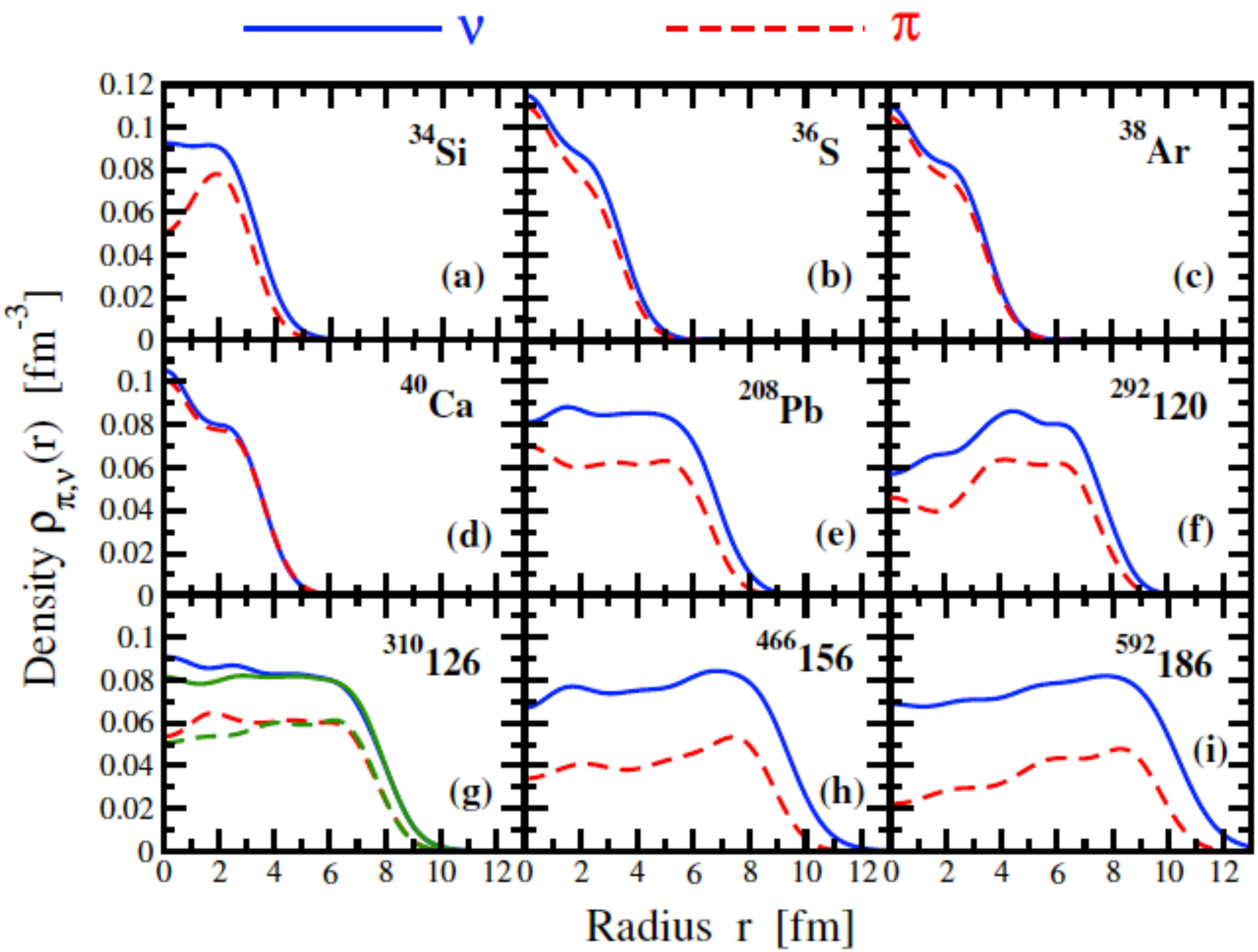

Question: How the deviations from flat densities in subsurface region affect the description of the HI collisions

Are the densities flat in the central part of the nucleus?

$$\rho_{tot}(r) = \sum_i (2j_i + 1)\rho_i^{sp}(r).$$

$$\int \rho_i^{sp}(r) d^3 r = 1.0$$

Microscopic origin of the peak in total densities at r=0: the occupation of the $s_{1/2}$ proton and neutron states.

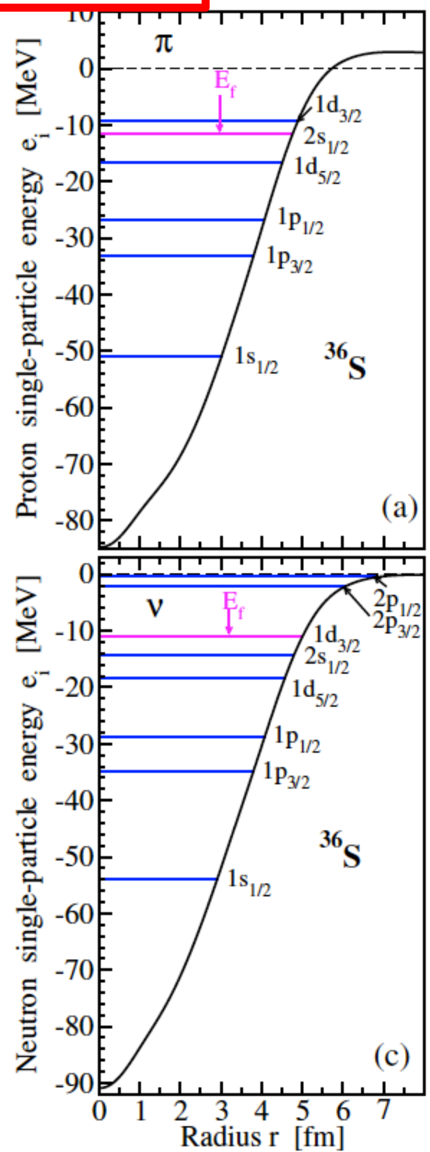

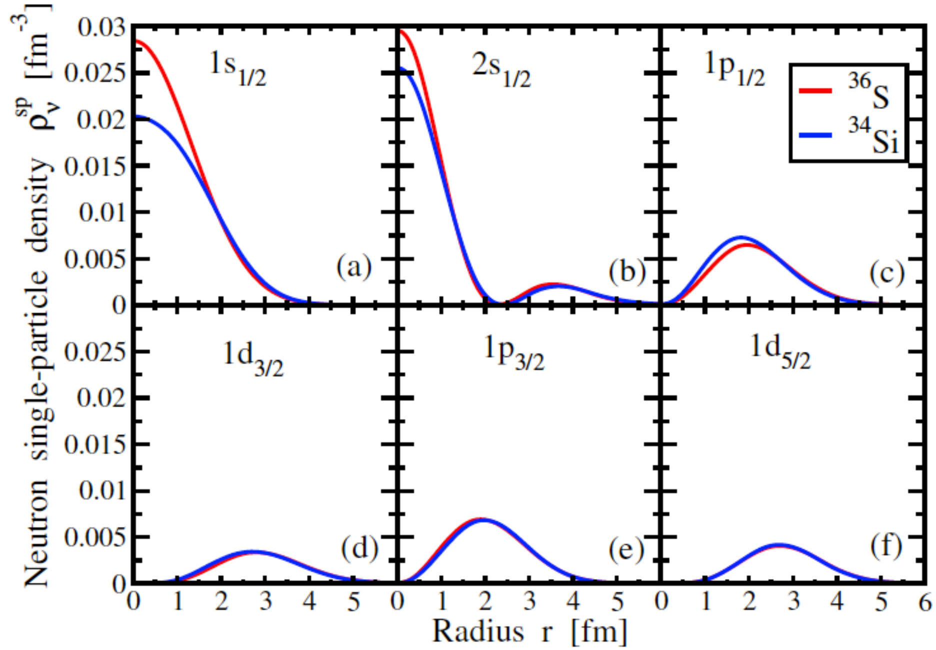

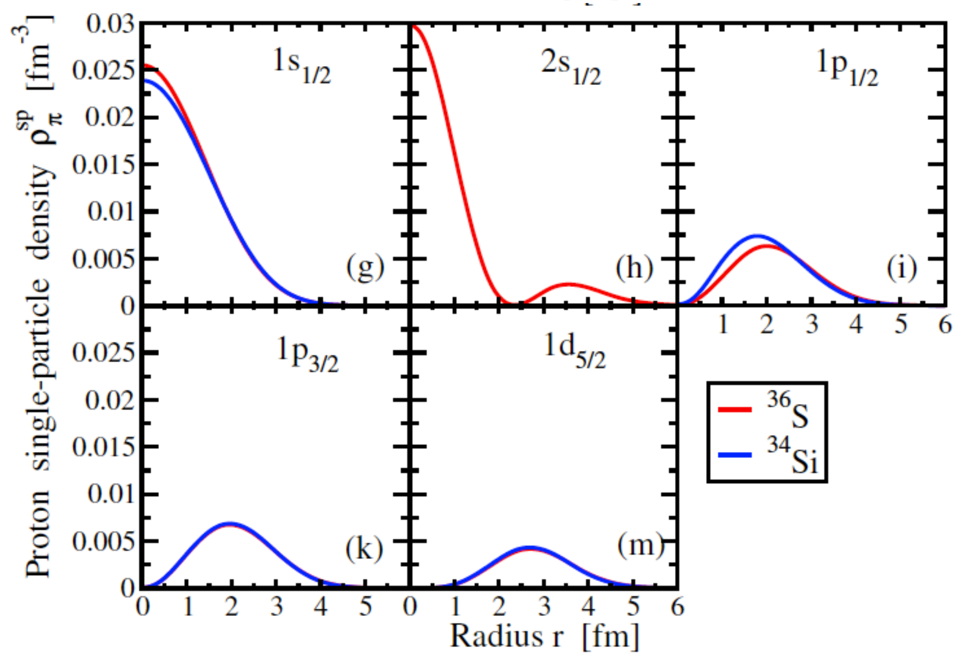

The toroidal shapes: distribution in nuclear chart and their stability with respect of breathing deformations

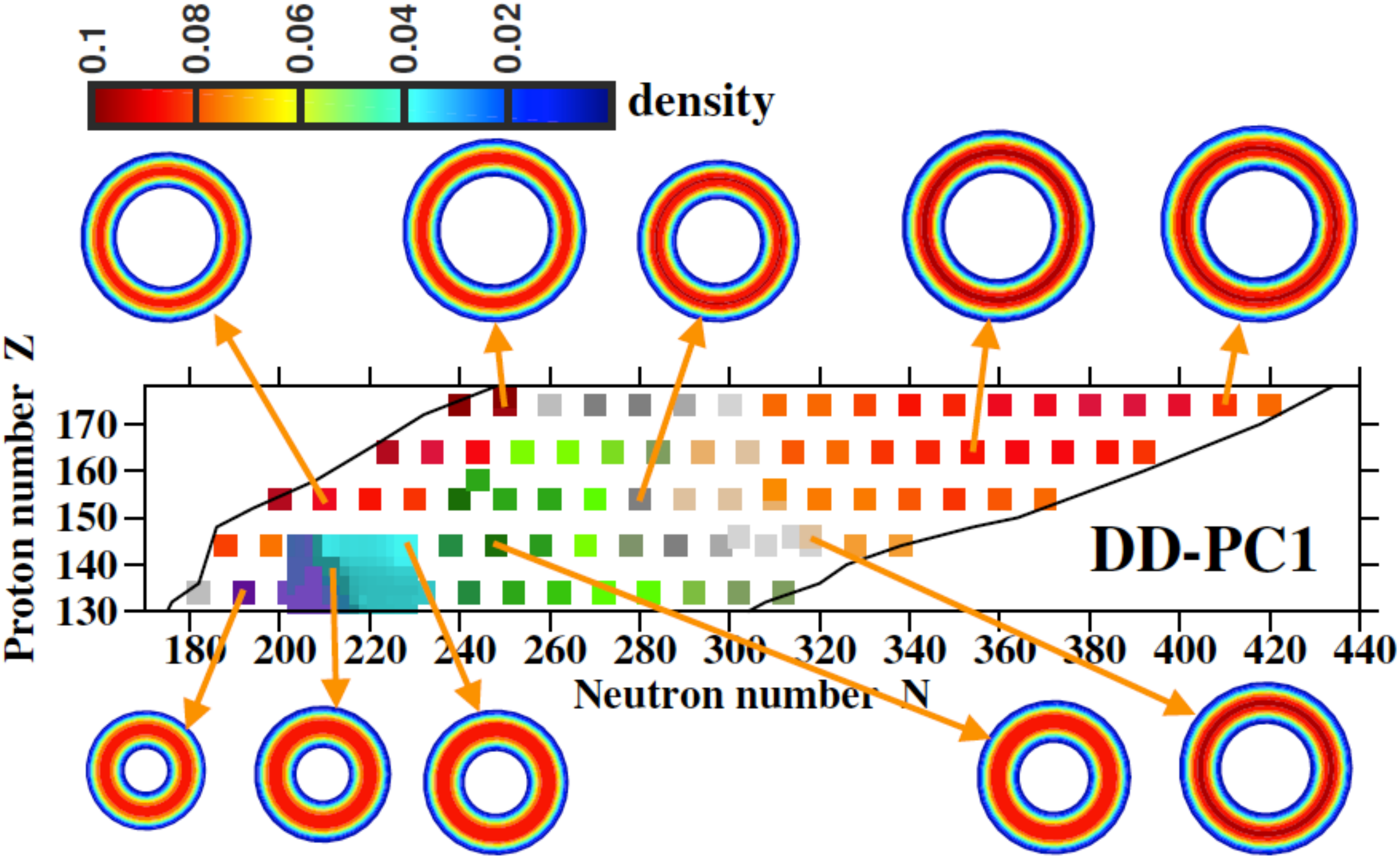

Toroidal nuclei are stable with respect of breathing deformations

Possible observation of toroidal shapes at high spin in ^{28}Si

X.G.Cao et al, PRC 99, 014606 (2019)

Examination of evidence for resonances at high excitation energy in the 7α disassembly of ^{28}Si

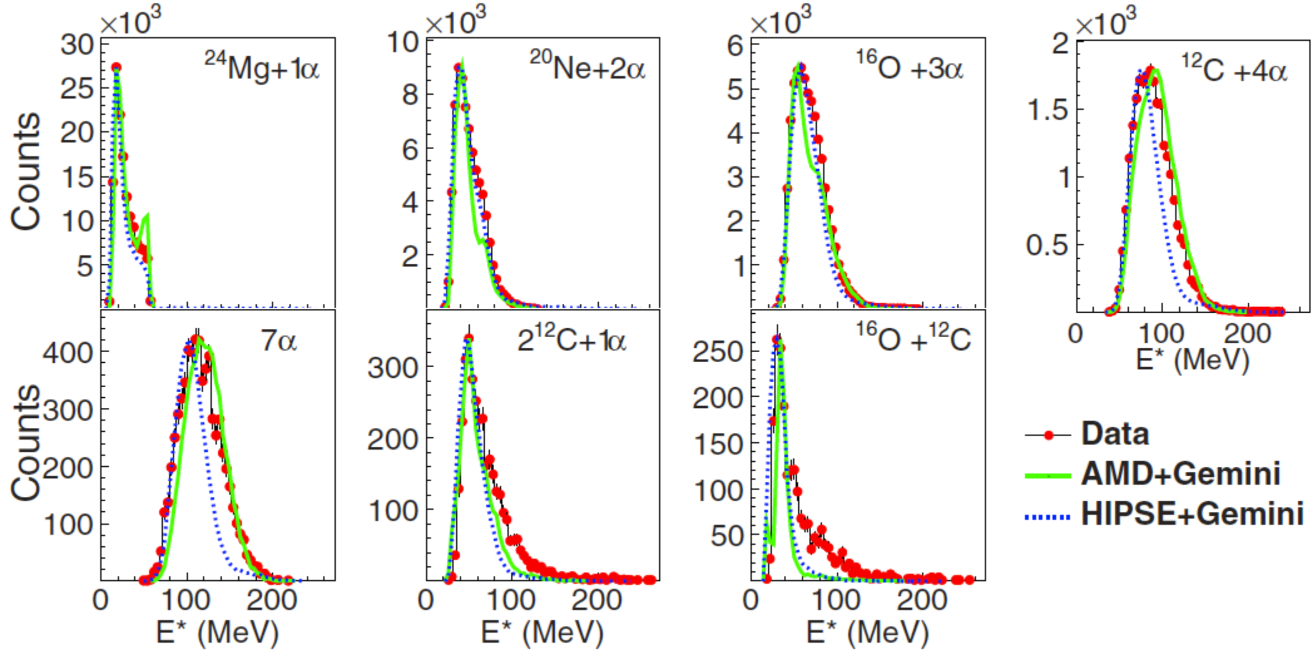

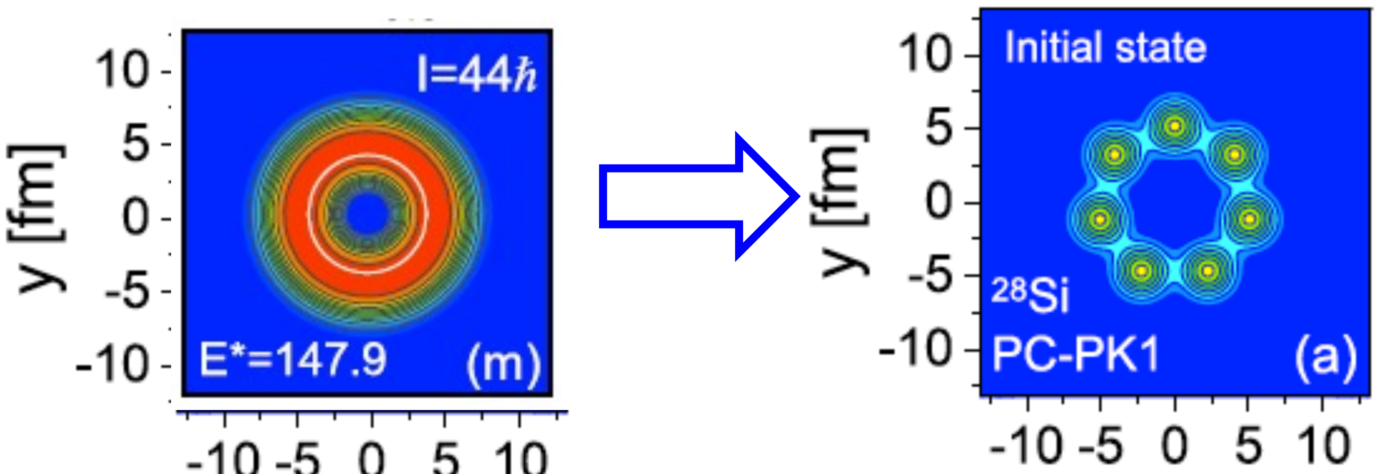

Z.X.Ren et al, NPA 996, 121696 (2020)

"Evidence for the Decay of Nuclear Matter Toroidal Geometries in Nucleus-Nucleus Collisions", N. T. B. Stone et al, PRL **78**, 2084 (1997)

$^{86}Kr + ^{93}Nb$ reactions

Open question: how to produce hyperheavy nuclei

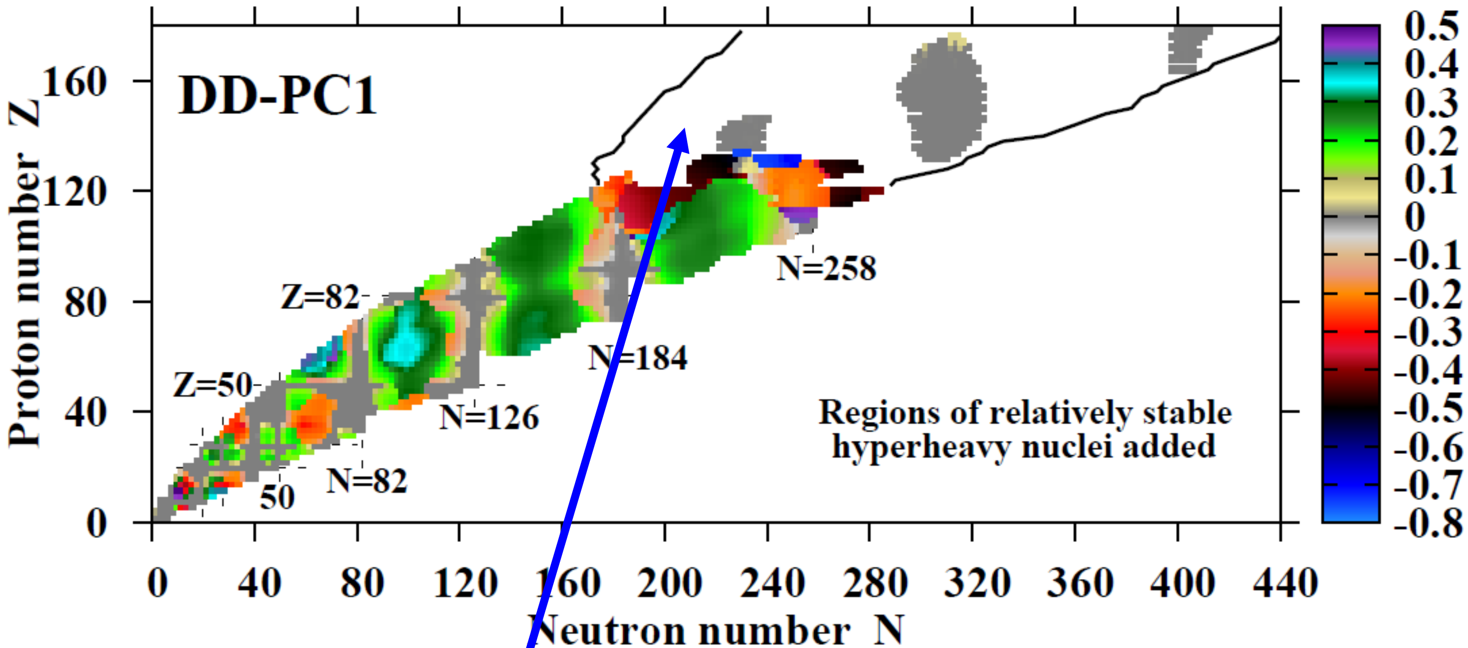

Fusion reactions of stable nuclei $^{116}Sn + ^{208}Pb$ gives the element with (Z=132,N=192)